

Exact asymptotic statistics of the n -edged face in a 3D Poisson-Voronoi tessellation

H. J. Hilhorst

Laboratoire de Physique Théorique, Bâtiment 210
Université Paris-Sud and CNRS
Université Paris-Saclay
91405 Orsay Cedex, France

March 6, 2022

Abstract

We consider the 3D Poisson-Voronoi tessellation. We investigate the joint probability distribution $\pi_n(L)$ for an arbitrarily selected cell face to be n -edged and for the distance between the seeds of its adjacent cells to be equal to $2L$. We derive an exact expression for this quantity, valid in the limit $n \rightarrow \infty$ with $n^{1/6}L$ fixed. The leading order correction term is determined. Good agreement with earlier Monte Carlo data is obtained. The cell face is surrounded by a three-dimensional excluded domain that is the union of n balls; it is pumpkin-shaped and analogous to the flower of the 2D Voronoi cell. For $n \rightarrow \infty$ this domain tends towards a torus of equal major and minor radii. The radii scale as $n^{1/3}$, in agreement with earlier heuristic work. We achieve a detailed understanding of several other statistical properties of the n -edged cell face.

Keywords: random graphs, Voronoi tessellations, exact results

1 Introduction

Let there be given a set of N point-like “seeds” in a domain of volume V in three-dimensional Euclidean space \mathbb{R}^3 . The Voronoi tessellation based on this set is the partitioning of space into cells, one around each seed, in such a way that every generic point of space is in the cell of the seed to which it is closest. If the seeds are randomly and uniformly distributed, the tessellation is called a Poisson-Voronoi tessellation. Obviously this construction is easily generalized to arbitrary spatial dimension.

Voronoi tessellations have applications across the sciences, whether as models that directly describe natural systems or as tools for data analysis. Many applications have been reviewed by Okabe *et al.* [1].

The exact statistics of Poisson-Voronoi cells has been a subject of investigation by physicists and mathematicians alike. Lists of exact results are given in Ref. [1] for tessellations of \mathbb{R}^2 and \mathbb{R}^3 . They refer to properties in the “thermodynamic limit”, that is, the limit $N, V \rightarrow \infty$ at fixed seed density $\lambda = N/V$. In this paper we derive new exact results in 3D. They concern the statistics of a face shared by two 3D cells, and in particular the limit in which the number of edges of that face becomes very large. The work builds on earlier results in 2D that we briefly summarize in the next subsection.

1.1 The 2D Poisson-Voronoi tessellation

In two-dimensional space a quantity of basic interest is the sidedness distribution $p_n^{(2)}$, that is, the probability for a two-dimensional Poisson-Voronoi cell to have exactly n sides. No simple exact closed-form expression is known for this elementary probability distribution.

About a decade ago we investigated [2, 3] the large n behavior of $p_n^{(2)}$ and found the asymptotic expansion of $\log p_n^{(2)}$ in inverse powers of n . One by-product of this calculation was an efficient algorithm [4] for simulating n -sided cells for large n . Another development [5] based on Ref. [3] dealt with the relation between a many-sided cell and its first-neighbor cells and led to the replacement of Aboav’s “linear law” by a square-root law.

The methods of Refs. [2, 3] proved to be applicable to at least two other two-dimensional geometric problems. The first application [6] is to a family of line tessellations introduced by Hug and Schneider [7]. The second application [8] is to “Sylvester’s question” [9]: if n random points are distributed uniformly in some convex subdomain of \mathbb{R}^2 , then what is the probability p_n^{Sylv} that they are the vertices of a convex n -gon? For the subdomain equal to the unit disk, Ref. [8] obtained the asymptotic expansion of $\log p_n^{\text{Sylv}}$.

In all these problems there appears a closed random curve that in the limit $n \rightarrow \infty$ tends to a circle while satisfying a stochastic ordinary linear second order differential equation known as the *random acceleration process* [10, 11, 12]. These interrelationships provide a motivation for the study of this paper, in which for the first time our methods are brought to bear on a 3D question.

1.2 The edgedness of a face between 3D cells

One immediate 3D generalization of the 2D sidedness distribution is the facedness probability $p_n^{(3)}$, that is, the probability that a three-dimensional Poisson-Voronoi cell have n faces. Again, this probability distribution is unknown and one might hope to find its asymptotic large- n behavior by the methods of Refs. [3, 6, 8]. However, we do not know how to solve that problem.

A different generalization of the 2D quantity $p_n^{(2)}$ to 3D is the probability – henceforth to be denoted for simplicity by p_n – that an arbitrarily chosen face shared by two 3D cells have exactly n edges. In this paper we will find the asymptotic expansion of $\log p_n$ for large n together with a large number of other statistical properties, summarized below.

This question about the edgedness distribution is richer than the one about the facedness. The facedness question involves a single 3D Voronoi cell and is, statistically, spherically symmetric. The edgedness question, however, involves two adjacent 3D cells (the “focal cells”) and only has rotational symmetry about the axis passing through the seeds of the two cells. The distance $2L$ between these seeds (where L is called the “focal distance”) enters the game as an extra parameter.

We will be naturally led to consider the joint probability distribution $\pi_n(L)dL$, defined as the probability that an arbitrarily chosen cell face have n edges and is shared by two cells whose focal distance is between L and $L+dL$. As a consequence

$$p_n = \int_0^\infty dL \pi_n(L). \quad (1.1)$$

We will also write

$$\pi_n(L) = Q_n(L)p_n, \quad (1.2)$$

where $Q_n(L)$ is the conditional probability that an n -edged cell face separate seeds of distance $2L$. The objects of interest in this paper are p_n and $Q_n(L)$, both in the limit of large n .

Earlier studies of the edgedness were performed by Kumar *et al.* [13] and more recently in Ref. [14], where the Monte Carlo work of Lazar *et al.* [15] was extended and a heuristic theory was presented to explain the results. In sections 12.2 and 12.3 we will compare our present results to these earlier studies.

1.3 Method

In section 2 the edgedness probability $\pi_n(L)$ is cast in the form of a phase space integral on the $3n$ position coordinates $\mathbf{R}_1, \mathbf{R}_2, \dots, \mathbf{R}_n$ in \mathbb{R}^3 of the first-neighbor seeds. This multiple integral is then analogous to the configurational partition function of a system of n interacting particles. The following sections are basically a concatenation of steps needed to evaluate this integral.

In section 3 we perform a transformation to new radial and polar coordinates. In section 4 we establish the shape of a 3D excluded domain which is analogous to

the “flower” of the 2D Voronoi cell. There are good reasons in our case to call this domain a “pumpkin.” We point out by geometrical considerations that there is an invariance allowing this 3D problem to be reduced to one in 2D. We do precisely that in section 5 by integrating over the polar angles. The techniques developed in Ref. [3] may then be adapted to the resulting 2D problem. In section 6 we perform further coordinate transformations that leave it as a problem of integrating on a single radial and $2n - 1$ angular variables. All these rewritings of the original problem are reversible and merely amount to a different representation of $\pi_n(L)$.

In section 7 we prepare for a large- n expansion of $\pi_n(L)$. Our strategy is to hypothesize, in subsection 7.1, the appropriate scaling with n of all variables of integration involved, and to show that these assumed scalings are consistent and lead to an expansion with finite coefficients. In subsections 7.2-7.4 we carry out the expansion of the various factors in the integrand in negative powers of n to the order required. In section 8 we perform the radial integration by means of a saddle point calculation. In sections 9, 10, and 11 we turn to the remaining integrals, which are those over the angular variables. Their calculation is analogous to the 2D problem [3] and we omit details. The work nevertheless goes beyond a simple analogy in two respects. First, the present problem has the extra parameter L ; and second, our calculation of $Q_n(L)$ includes the next-to-leading terms, which are of relative order n^{-1} . It will appear that these correction terms greatly enhance the agreement with the simulations.

In section 12 we combine all preceding relations to arrive at the final results. In section 13 we briefly conclude.

The calculation of this paper is of considerable length, even with our omitting details that may be found in earlier papers. However, only standard methods of mathematical analysis are used.

Since the subject matter of this work has attracted much activity among mathematicians, the following remark may be appropriate. We present our methods and results as “exact,” and they certainly are by the usual standards of theoretical physics. They are based on a formal expansion without, however, the necessary proofs that the higher order terms are actually negligible for $n \rightarrow \infty$. We are well aware that this procedure is not rigorous and fully accept that mathematicians consider our results as conjectures.

1.4 Results

The main results of this work are the following.

(i) In the large- n limit the n -edged face tends towards a circle whose random radius is narrowly peaked around

$$R_n \simeq (2\pi^2\lambda)^{-1/3}n^{1/3}, \quad n \rightarrow \infty. \quad (1.3)$$

Here and throughout the symbol \simeq will indicate asymptotic equality.

(ii) The leading order behavior of p_n is

$$p_n = \frac{1}{c_F} \left(\frac{3}{2\pi^5 n} \right)^{1/2} \frac{(12\pi^2)^n}{(2n)!} C(3) [1 + \mathcal{O}(n^{-1})] \quad (1.4)$$

in which $c_F = 48\pi^2/35 + 2 = 15.535$ is the average number of faces of a cell [1] and $C(3)$ is a constant given by

$$C(3) = \prod_{q=1}^{\infty} \frac{q^4}{q^4 + 9} = 0.053891. \quad (1.5)$$

This constant may be interpreted as the partition function of the elastic degrees of freedom of the face,¹ each factor in the product representing the contribution of a Fourier mode of a definite wavenumber. A similar constant was found in our study [3] of the sidedness probability $p_n^{(2)}$ of the 2D cell.

(iii) The conditional probability distribution $Q_n(L)$ defined in (1.2) may be expressed with the aid of the scaling variable

$$y \equiv \kappa n^{1/6} L, \quad \kappa = 2^{-1/6} 3^{-1/2} \pi^{7/6} \lambda^{1/3}. \quad (1.6)$$

In the limit $n \rightarrow \infty$ at fixed y we have

$$Q_n(L) = \kappa n^{1/6} \mathcal{Q}(y) \left[1 + \frac{q_2 y^2 + q_4 y^4 - q_0}{n} + \mathcal{O}(n^{-2}) \right]. \quad (1.7)$$

with

$$\mathcal{Q}(y) = \frac{32}{\pi^2} \exp\left(-\frac{4y^2}{\pi}\right), \quad y > 0. \quad (1.8)$$

The coefficients q_i in (1.7) have explicit analytic expressions, given in section 12, whose numerical values are $q_2 = 3.71726$, $q_4 = 0.36025$, and $q_0 = 5.21263$. In section 12.3 we compare (1.7) to the Monte Carlo results of Ref. [14] and find good qualitative agreement.

(iv) It follows that for an n -edged face the average value of L , to be denoted by \mathbb{L}_n , is given by

$$\mathbb{L}_n = \frac{1}{\kappa n^{1/6}} \left[1 + \frac{l_1}{n} + \mathcal{O}(n^{-2}) \right] \quad (1.9)$$

with an analytic expression for l_1 given in section 12 whose numerical value is $l_1 = 1.95558$. The proportionality to $n^{-1/6}$ that appears in (1.9) may be seen as an attraction of entropic origin between the two focal seeds. Comparison of (1.9) to the Monte Carlo results of Ref. [14] shows again good agreement.

(v) We denote as *first-neighbor seeds* those whose cells share an edge of the face between the two focal cells. The first-neighbor seeds lie in a shell whose width tends to zero for $n \rightarrow \infty$ and whose shape tends to the surface of a spindle torus of major radius R_n and minor radius $S_n = \sqrt{R_n^2 - \mathbb{L}_n^2}$. In the limit $n \rightarrow \infty$ this spindle torus becomes a torus with equal major and minor radius (a “horn torus”).

¹*I.e.*, the deviations of the face boundary from circularity. This “elasticity” is of course of purely entropic origin.

2 The n -edged face and the focal distance L

2.1 The joint probability $\pi_n(L)$

We consider a Poisson-Voronoi tessellation in three-dimensional space, constructed from N seeds having positions $\mathbf{R}_1, \mathbf{R}_2, \dots, \mathbf{R}_N$ that are independently and uniformly distributed in a domain of volume V . At appropriate points in the calculation we will let $N, V \rightarrow \infty$ with the seed density $\lambda = N/V$ fixed. We may scale λ to unity but will keep it in the formulas a dimensional check.

We select an arbitrary cell face. It is known [1] that for $N, V \rightarrow \infty$ a cell has on average

$$c_F = \frac{48\pi^2}{35} + 2 = 15.535 \quad (2.1)$$

faces. Since each face belongs to a unique pair of neighboring cells, selecting a cell face uniformly among all $\frac{1}{2}Nc_F$ faces amounts to selecting a cell pair (i, j) uniformly among all $\frac{1}{2}N(N-1)$ cell pairs and retaining it only if i and j are neighbors. The probability P for retention is therefore

$$P \simeq \frac{c_F}{N}, \quad N \rightarrow \infty. \quad (2.2)$$

We may decompose P according to

$$P = \int_0^\infty dL \sum_{n=3}^\infty P_n(L), \quad (2.3)$$

in which $P_n(L)dL$ is the probability that i and j be neighbors, that the face they share be n -edged, and that their focal distance (half the distance between their seeds) be between L and $L + dL$. Hence

$$\pi_n(L)dL = \frac{P_n(L)}{P}dL \quad (2.4)$$

is the probability that an arbitrarily selected cell face be n -edged and that the two cells sharing it have a focal distance between L and $L + dL$. The normalization is

$$\int_0^\infty dL \sum_{n=3}^\infty \pi_n(L) = 1. \quad (2.5)$$

Our interest is in this quantity $\pi_n(L)$. Eqs.(1.1) and (1.2) show how we may decompose it into the probability p_n that the interface have n edges and the conditional probability $Q_n(L)$ that the focal distance associated with an n -edged face be equal to L .

2.2 The probability $\pi_n(L)$ as a $3n$ -fold integral

Since the probability P is the same for all (i, j) , we will take for definiteness $(i, j) = (N-1, N)$. We can find an expression for $P_n(L)$ by writing P as an integral over all seed configurations and inserting the appropriate indicator function

$\chi_n(\mathbf{R}_1, \dots, \mathbf{R}_{N-2}; \mathbf{R}_{N-1}, \mathbf{R}_N)$ which is unity if cells $N-1$ and N share an n -edged face and vanishes otherwise. We get

$$P = \frac{1}{V^N} \int_V d\mathbf{R}_1 \dots d\mathbf{R}_N \sum_{n=3}^{\infty} \chi_n(\mathbf{R}_1, \dots, \mathbf{R}_{N-2}; \mathbf{R}_{N-1}, \mathbf{R}_N). \quad (2.6)$$

Obviously χ_n can depend on the seed positions \mathbf{R}_{N-1} and \mathbf{R}_N only through their distance $|\mathbf{R}_{N-1} - \mathbf{R}_N| \equiv 2L$. We may therefore fix these seeds at $\mathbf{R}_{N-1} = \mathbf{L}_1 \equiv (0, 0, L)$ and $\mathbf{R}_N = \mathbf{L}_2 \equiv (0, 0, -L)$ while replacing the integration $\int_V d\mathbf{R}_{N-1} d\mathbf{R}_N$ by $4\pi V \int_0^\infty (2L)^2 d(2L)$. Eq. (2.6) then becomes

$$P = \frac{32\pi}{V^{N-1}} \int_V d\mathbf{R}_1 \dots d\mathbf{R}_{N-2} \int dL L^2 \sum_{n=3}^{\infty} \chi_n(\mathbf{R}_1, \dots, \mathbf{R}_{N-2}; L), \quad (2.7)$$

where the last argument in χ_n is now meant as a reminder that $\mathbf{R}_{N-1} = \mathbf{L}_1$ and $\mathbf{R}_N = \mathbf{L}_2$. The face shared by the two cells now lies in the xy plane.

Each edge of the face is shared by the two focal cells and a third cell that we will refer to as *first-neighbor cell*; we will call its seed a *first-neighbor seed*. There are $\binom{N-2}{n}$ equivalent ways of choosing the n first-neighbor seeds among the $N-2$ seeds over whose positions we integrate in (2.7). By a permutation of indices we may take the first neighbors to be those of coordinates $\mathbf{R}_1, \mathbf{R}_2, \dots, \mathbf{R}_n$ and compensate by an extra factor $\binom{N-2}{n}$ in the expression for P .

For each $j = 1, 2, \dots, N-2$, the two planes that perpendicularly bisect $L_1 R_j$ and $L_2 R_j$ ² also cut the xy plane in a common line that we will call ℓ_j .

We split χ_n according to

$$\chi_n(\mathbf{R}_1, \dots, \mathbf{R}_{N-2}; L) = \chi(\mathbf{R}_1, \mathbf{R}_2, \dots, \mathbf{R}_n; L) \prod_{j=n+1}^{N-2} \bar{\chi}(\mathbf{R}_j | \mathbf{R}_1, \dots, \mathbf{R}_n; L) \quad (2.8)$$

in which the first factor on the RHS contains the conditions on $\mathbf{R}_1, \dots, \mathbf{R}_n$, and the product the conditions on the remaining seed positions; explicitly

(i) $\chi(\mathbf{R}_1, \dots, \mathbf{R}_n; L)$ is unity if the ℓ_m with $m = 1, 2, \dots, n$ enclose a convex n -gon (which is then the face; see Fig. 1), and is zero otherwise;

(ii) $\bar{\chi}(\mathbf{R}_j | \mathbf{R}_1, \dots, \mathbf{R}_n; L)$ is unity if the perpendicular bisecting plane of $L_1 R_j$ (and hence also the one of $L_2 R_j$) intersects the xy plane along a line ℓ_j that does not cut the face. This will be true if and only if \mathbf{R}_j stays outside a three-dimensional domain $\mathcal{V}(\mathbf{R}_1, \dots, \mathbf{R}_n; L)$ determined uniquely by the positions of the two focal seeds and the n first-neighbor seeds. We will find an explicit characterization of this domain later; its volume will be denoted by \mathcal{V} .

When inserting (2.8) in (2.7) and integrating over $\mathbf{R}_{n+1}, \dots, \mathbf{R}_{N-2}$ we get

$$P = \frac{32\pi}{V^{N-1}} \int dL L^2 \sum_{n=3}^{\infty} \binom{N-2}{n} \int d\mathbf{R}_1 \dots d\mathbf{R}_n \chi(\mathbf{R}_1, \dots, \mathbf{R}_n; L) \times [V - \mathcal{V}(\mathbf{R}_1, \dots, \mathbf{R}_n; L)]^{N-2-n}. \quad (2.9)$$

²We write AB for the line segment connecting the points \mathbf{A} and \mathbf{B} , and will write \overline{AB} for its length.

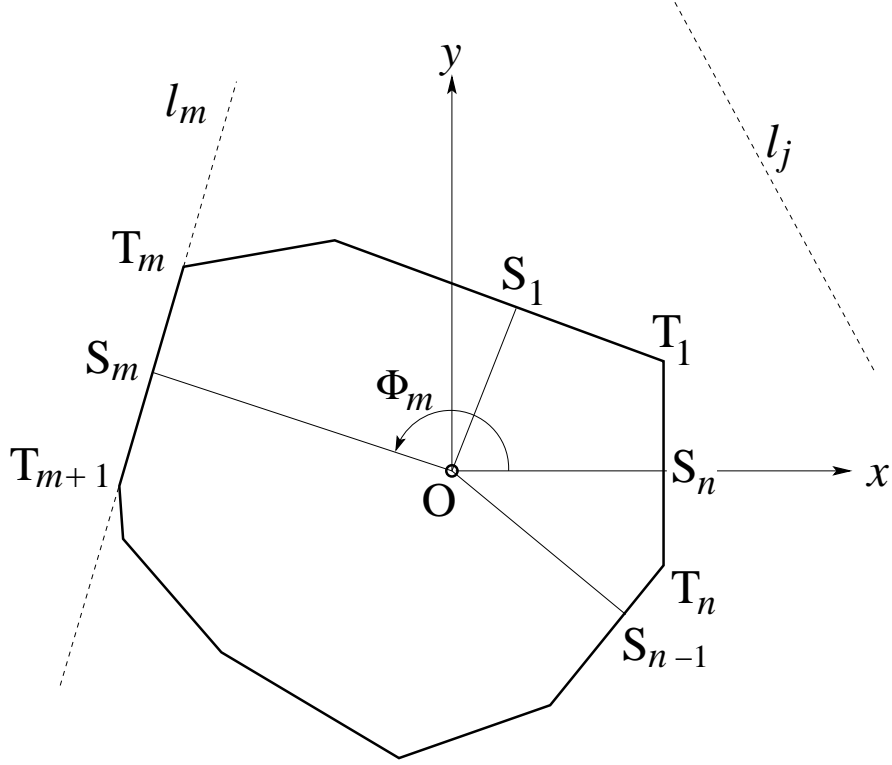


Figure 1: Geometry in the xy plane. The n -sided face between two adjacent cells has vertices $\mathbf{T}_1, \mathbf{T}_2, \dots, \mathbf{T}_n$. The lines ℓ_j for $j = 1, 2, \dots, N - 2$ are defined in section 2.2. The edges of the face lie on the ℓ_m with $m = 1, 2, \dots, n$. The ℓ_j with $n + 1, n + 2, \dots, N - 2$ do not intersect the face.

Upon comparing (2.9) and (2.3) we identify $P_n(L)$. We now multiply both members of (2.9) by N , use (2.4) and (2.2), and take the limit $N, V \rightarrow \infty$ at fixed $\lambda = N/V$. This leads to

$$\pi_n(L) = \frac{32\pi\lambda^{n+1}}{c_F} \frac{L^2}{n!} \int d\mathbf{R}_1 \dots d\mathbf{R}_n \chi(\mathbf{R}_1, \dots, \mathbf{R}_n; L) e^{-\lambda V(\mathbf{R}_1, \dots, \mathbf{R}_n; L)}. \quad (2.10)$$

With equation (2.10) we have achieved expressing $\pi_n(L)$ as a $3n$ -fold integral.

Before embarking upon the explicit evaluation of (2.10) we pass to spherical coordinates $\mathbf{R}_m = (R_m, \Phi_m, \Theta_m)$ defined as follows. As usual, R_m is the length of \mathbf{R}_m and Φ_m is the azimuthal angle, measured with respect to the positive x axis; however, in deviation from standard usage, the polar angle Θ_m will be measured from the xy plane in the direction of the positive z axis; that is, we have $-\frac{\pi}{2} \leq \Theta_m \leq \frac{\pi}{2}$. This definition allows us to maintain an explicit symmetry between the two half-spaces above and below the plane of the face. Eq. (2.10) then transforms into

$$\begin{aligned} \pi_n(L) = & \frac{32\pi\lambda^{n+1}}{c_F} \frac{L^2}{n!} \int_0^\infty \prod_{m=1}^n dR_m R_m^2 \int_{-1}^1 \prod_{m=1}^n d\sin \Theta_m \\ & \times \int_0^{2\pi} \prod_{m=1}^n d\Phi_m \chi(\mathbf{R}_1, \dots, \mathbf{R}_n; L) e^{-\lambda V(\mathbf{R}_1, \dots, \mathbf{R}_n; L)}. \end{aligned} \quad (2.11)$$

We consider this $3n$ -fold integral for $\pi_n(L)$ as the starting point of this paper. Our purpose will be to render it more explicit and to extract from it the most interesting information that it contains.

3 Coordinates in the m th first-neighbor plane

3.1 Geometry

Let us suppose for convenience that $m = 1, 2, \dots, n$ numbers the edges of the face in counterclockwise order.³ In the xy plane, let \mathbf{S}_m be the projection of the origin \mathbf{O} onto ℓ_m ; this point may lie on the m th edge of the face or on its extension (see figure 1). It is equidistant to the three seeds \mathbf{L}_1 , \mathbf{L}_2 , and \mathbf{R}_m , and lies in the plane passing through these seeds, which we will call the m th *first-neighbor plane* (see figure 2). We write r_m for the radius of the circle of center \mathbf{S}_m that passes through these three seeds. Since the set of projections $\{\mathbf{S}_m | m = 1, 2, \dots, n\}$ completely determines the face, we will refer it as the set of *face coordinates*.

3.2 Coordinate transformation

In the m th first-neighbor plane the coordinates R_m and Θ_m identify the m th first-neighbor seed. We will now prepare for integrating over these coordinates. To that end we will transform them to coordinates s_m and θ_m defined in figure 2. We do this in two steps: first from (R_m, Θ_m) to (r_m, θ_m) and then from r_m to s_m .

³This may be achieved by a permutation of the indices $1, 2, \dots, n$; see section 6.2.

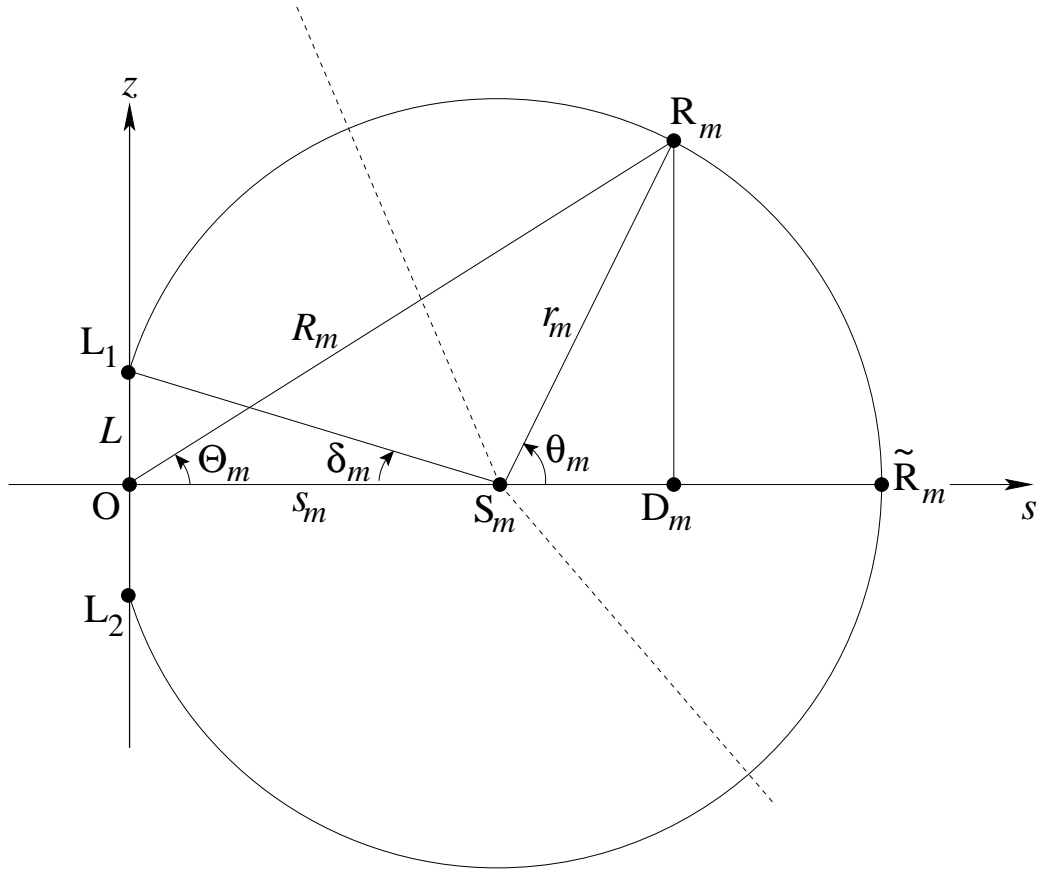


Figure 2: The m th first-neighbor plane contains the seeds \mathbf{L}_1 , \mathbf{L}_2 , and \mathbf{R}_m . The three corresponding cells share pairwise three faces whose intersections with the plane of the figure lie on the two dashed lines (the perpendicular bisectors of L_1R_m and L_2R_m) and the s axis (perpendicular bisector of L_1L_2).

3.2.1 From (R_m, Θ_m) to (r_m, θ_m)

To find the transformation we observe that $\overline{D_m R_m}$ may be calculated in the triangles $OD_m R_m$ and $C_m D_m R_m$, which yields

$$R_m \sin \Theta_m = r_m \sin \theta_m. \quad (3.1)$$

Furthermore the relation $\overline{OD_m} = \overline{OC_m} + \overline{C_m D_m}$ may be expressed as

$$\begin{aligned} R_m \cos \Theta_m &= \sqrt{r_m^2 - L^2} + r_m \cos \theta_m \\ &= r_m [\cos \delta_m + \cos \theta_m], \end{aligned} \quad (3.2)$$

where we introduced the abbreviation

$$\cos \delta_m = \sqrt{1 - L^2/r_m^2}. \quad (3.3)$$

From (3.1) and (3.2) one deduces for R_m^2 and $\sin^2 \Theta_m$ the following explicit expressions in terms of the new coordinates

$$\begin{aligned} R_m^2 &= 2r_m^2 - L^2 + 2r_m^2 \cos \delta_m \cos \theta_m, \\ \sin^2 \Theta_m &= \frac{r_m^2 \sin^2 \theta_m}{2r_m^2 - L^2 + 2r_m^2 \cos \delta_m \cos \theta_m}. \end{aligned} \quad (3.4)$$

We will need the Jacobian $J_m = \partial(R_m, \sin \Theta_m) / \partial(r_m, \sin \theta_m)$ of this transformation.

3.2.2 The Jacobian J_m

To calculate the Jacobian J_m we abbreviate

$$R_{mr} = \frac{\partial R_m}{\partial r_m}, \quad R_{m\theta} = \frac{\partial R_m}{\partial \sin \theta_m}, \quad \Theta_{mr} = \frac{\partial \sin \Theta_m}{\partial r_m}, \quad \Theta_{m\theta} = \frac{\partial \sin \Theta_m}{\partial \sin \theta_m}. \quad (3.5)$$

Upon deriving Eqs. (3.1) and (3.2) with respect to r_m and $\sin \theta_m$ we get the four equations

$$\begin{aligned} R_{mr} \sin \Theta_m + \Theta_{mr} R_m &= \sin \theta_m, \\ R_{m\theta} \cos \Theta_m - \Theta_{m\theta} R_m \tan \Theta_m &= \frac{1}{\sqrt{1 - L^2/r_m^2}} + \cos \theta_m, \end{aligned} \quad (3.6)$$

$$\begin{aligned} R_{m\theta} \sin \Theta_m + \Theta_{m\theta} R_m &= r_m, \\ R_{m\theta} \cos \Theta_m - \Theta_{m\theta} R_m \tan \Theta_m &= -r_m \tan \theta_m. \end{aligned} \quad (3.7)$$

We may solve R_{mr} and Θ_{mr} from Eqs. (3.6) and $R_{m\theta}$ and $\Theta_{m\theta}$ from Eqs. (3.7). After some algebra this yields

$$\begin{aligned} J_m &= R_{mr} \Theta_{m\theta} - R_{m\theta} \Theta_{mr} \\ &= \frac{r_m \cos \Theta_m}{R_m} \left[\frac{1}{\cos \theta_m} + \frac{1}{\sqrt{1 - L^2/r_m^2}} \right] \\ &= \frac{\cos^2 \Theta_m}{\cos \theta_m \cos \delta_m}, \end{aligned} \quad (3.8)$$

where to arrive at the last line we used (3.2).

In the integral in (2.11) this change of variables of integration therefore leads to the transformation

$$\begin{aligned}
dR_m R_m^2 d\sin\Theta_m &= dr_m d\sin\theta_m J_m R_m^2 \\
&= dr_m r_m^2 d\sin\theta_m \frac{(\cos\delta_m + \cos\theta_m)^2}{\cos\delta_m \cos\theta_m} \\
&= dr_m r_m^2 d\theta_m \left(1 - \frac{L^2}{r_m^2}\right)^{-\frac{1}{2}} \left[\left(1 - \frac{L^2}{r_m^2}\right)^{\frac{1}{2}} + \cos\theta_m\right]^2,
\end{aligned} \tag{3.9}$$

where to pass from the first to the second line we used (3.2) and (3.8).

3.2.3 From r_m to s_m

We set

$$s_m^2 = r_m^2 - L^2 \tag{3.10}$$

and refer again to figure 2. We then find from Eq. (3.9) that

$$dR_m R_m^2 d\sin\Theta_m = ds_m s_m^2 d\theta_m \left[1 + \frac{\cos\theta_m}{\cos\delta_m}\right]^2 \tag{3.11}$$

where now

$$\frac{1}{\cos\delta_m} = \sqrt{1 + \frac{L^2}{s_m^2}}. \tag{3.12}$$

It may be noted that for $\delta_m \rightarrow \pi/2$ the divergence of the bracketed factor in (3.11) is compensated by the fact that in that limit $s_m \rightarrow 0$.

3.2.4 Range of s_m and θ_m

When the first-neighbor position \mathbf{R}_m is integrated over the m th first-neighbor half-plane (that is, at fixed angle Φ_m), it will also run through the half-disk of center \mathbf{O} and radius L that is part of this half-plane. In that case the center \mathbf{S}_m moves into the complementary half-plane, which we may express by letting the coordinate s_m (see figure 2) be the negative square root of (3.10) and δ_m the angle between the negative s axis and OL_1 . This corresponds to the origin \mathbf{O} lying outside the cell face and to the azimuthal angle of \mathbf{S}_m being equal to $\Phi_m + \pi$. For large n the relative weight of this special subclass of faces will be exponentially small in n , and therefore negligible once we expand in powers of n in sections 7 through 12. It will be convenient to suppress this subclass from here on and let the new variables s_m and θ_m range through

$$0 < s_m < \infty, \quad -\pi + \delta_m < \theta_m < \pi - \delta_m, \tag{3.13}$$

with δ_m given in terms of s_m by (3.12). Eq. (2.11) may then be rewritten as

$$\begin{aligned} \pi_n(L) \simeq & \frac{32\pi\lambda^{n+1}}{c_F} \frac{L^2}{n!} \int_0^\infty \prod_{m=1}^n ds_m s_m^2 \int \prod_{m=1}^n d\theta_m \left[1 + \frac{\cos \theta_m}{\cos \delta_m} \right]^2 \\ & \times \int_0^{2\pi} \prod_{m=1}^n d\Phi_m \chi(\mathbf{R}_1, \dots, \mathbf{R}_n; L) e^{-\lambda \mathcal{V}(\mathbf{R}_1, \dots, \mathbf{R}_n; L)}, \end{aligned} \quad (3.14)$$

in which the limits of the θ_m integrations, not explicitly indicated, are those of Eq. (3.13); and where δ_m is given by (3.12).

We will now show that χ and \mathcal{V} are independent of the angles θ_m and that therefore the θ_m integrations in (3.14) are mutually independent and may be carried out fully explicitly.

4 The excluded domain \mathcal{V}

For given focal seeds in $\mathbf{L}_{1,2} = (0, 0, \pm L)$ and a given set of first-neighbor positions $\{\mathbf{R}_1, \dots, \mathbf{R}_n\}$, the domain $\mathcal{V}(\mathbf{R}_1, \dots, \mathbf{R}_n; L)$ is the region of space from which the remaining seeds are excluded if they are not to interfere with the first-neighbor relations. If one of those remaining seeds entered the excluded domain, it would itself become a first neighbor, contrary to what had been supposed. In this section we will obtain an explicit characterization of the excluded domain $\mathcal{V}(\mathbf{R}_1, \dots, \mathbf{R}_n; L)$. It will appear that it in fact depends only on the more restricted set of face coordinates $\{\mathbf{S}_1, \dots, \mathbf{S}_n\}$, that are all located in the xy plane. This feature will allow us to explicitly carry out the integrations over the angles θ_m .

4.1 Geometry in the half-plane at angle Φ

Let \mathbf{R}' be the position of an arbitrary one of the remaining seeds \mathbf{R}_j (where $j = n+1, \dots, N-2$) and let Φ be its azimuthal angle. Let furthermore ℓ_j be the line along which the perpendicular bisecting planes of $L_1 R'$ and of $L_2 R'$ intersect the xy plane; and let \mathbf{S}' be the projection of the origin \mathbf{O} onto ℓ' .

The considerations that follow all concern the vertical half-plane passing through the z axis and \mathbf{R}' , and that we will refer to as the *half-plane at angle Φ* . This half-plane contains \mathbf{S}' .

We have the following property. Let $r' \equiv \overline{S'R'}$. When in this half-plane \mathbf{R}' moves along a circular arc of center \mathbf{S}' and radius r' , having its end points in \mathbf{L}_1 and \mathbf{L}_2 , then ℓ' remains invariant. That is, in this half-plane this circular arc is a locus of positions \mathbf{R}' that are equivalent in the sense of leading to the same ℓ' . We will refer to this arc as arc $L_1 R' L_2$ and denote its intersection with the xy plane by $\tilde{\mathbf{R}}'$.

We wish to investigate under which conditions $\tilde{\mathbf{R}}'$ (and therefore any other point on the circular arc to which it belongs) is such that ℓ' does not cut the n -edged face; under these conditions $\tilde{\mathbf{R}}'$ is outside the excluded domain \mathcal{V} .

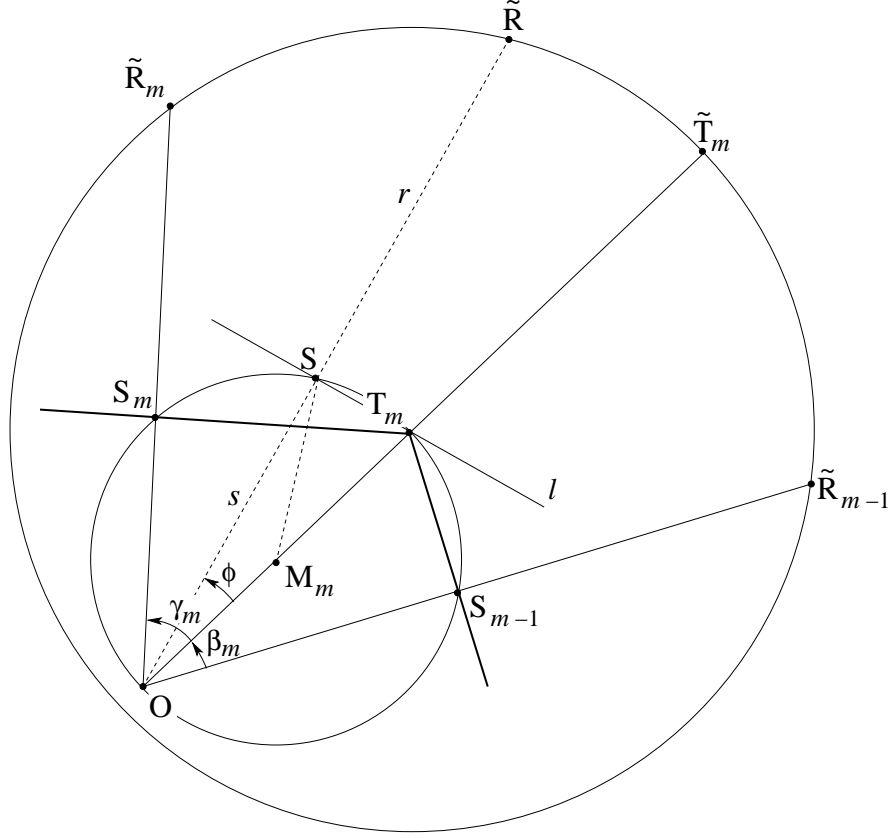


Figure 3: More geometry in the xy plane. The large circle has \mathbf{T}_m and the small one \mathbf{M}_m as its center. This figure defines the angles β_m , γ_m , and ϕ . We define $\xi_m = \beta_m + \gamma_m$ and $\eta_m = \gamma_m + \beta_{m+1}$ (n -periodicity understood). When \mathbf{S}_{m-1} (or \mathbf{S}_m) lies on the extension of the $(m-1)$ th (or the m th) edge beyond the point \mathbf{T}_m , then β_m (or γ_m) is negative. When ϕ varies from $-\beta_m$ to γ_m , point \mathbf{S} moves along the smaller circle from \mathbf{S}_{m-1} to \mathbf{S}_m and line ℓ pivots around \mathbf{T}_m ; $\tilde{\mathbf{R}}$ moves along the large circle from $\tilde{\mathbf{R}}_{m-1}$ to $\tilde{\mathbf{R}}_m$.

Suppose ℓ' cuts the face. Let us then move seed \mathbf{R}' in such a way that the bisector plane of $L_1\tilde{R}$ moves parallel to itself away from \mathbf{L}_1 .⁴ This means that in the xy plane along the half-axis at angle Φ the position $\tilde{\mathbf{R}}'$ and the center \mathbf{S}' move away from the origin while being related by

$$L^2 + s'^2 = r'^2, \quad \tilde{R}' = s' + r', \quad (4.1)$$

in which $s' = \overline{OS'}$ and $r' = \overline{S'\tilde{R}'} = \overline{S'R'}$. Line ℓ' will stop cutting the face when it passes only through a single vertex; if Φ is in the sector $\Phi_{m-1} < \Phi < \Phi_m$, this will be vertex \mathbf{T}_m . This is the situation is represented in figure 3, where we have denoted by ℓ , \mathbf{S} , and $\tilde{\mathbf{R}}$ (without primes) the positions then occupied by ℓ' , \mathbf{S}' , and $\tilde{\mathbf{R}}'$, respectively. Setting $s \equiv \overline{OS}$ and $r \equiv \overline{S\tilde{R}}$ we have from Eq. (4.1) that s and r are related by

$$L^2 + s^2 = r^2, \quad \tilde{R} = s + r. \quad (4.2)$$

The two equations (4.2) contain three unknowns s , r , and \tilde{R} that we would like to determine in terms of the running angle Φ and the face coordinates $\{\mathbf{S}_1, \dots, \mathbf{S}_n\}$. The third equation comes from the condition that ℓ pass through \mathbf{T}_m . We use the angles β_m , γ_m , and ϕ defined in figure 3. Here the auxiliary angle $\phi \equiv \Phi - \Phi_m$ is the “local” azimuthal angle in the m th sector and has the range

$$-\beta_m < \phi < \gamma_m. \quad (4.3)$$

Since $s = \overline{OT_m} \cos \phi$ and since for $\overline{OT_m}$ we may use either of the two expressions $\overline{OT_m} = s_{m-1}/\cos \beta_m = s_m/\cos \gamma_m$, it follows that

$$s(\phi) = s_{m-1} \frac{\cos \phi}{\cos \beta_m} = s_m \frac{\cos \phi}{\cos \gamma_m}. \quad (4.4)$$

The first one of Eqs. (4.2) then gives $r(\phi)$ as

$$r(\phi) = s_{m-1} \left(\frac{\cos^2 \phi}{\cos^2 \beta_m} + \frac{L^2}{s_{m-1}^2} \right)^{1/2} = s_m \left(\frac{\cos^2 \phi}{\cos^2 \gamma_m} + \frac{L^2}{s_m^2} \right)^{1/2}. \quad (4.5)$$

Eqs. (4.4) and (4.5) are both valid in the m th sector, that is, for $\Phi_{m-1} < \Phi < \Phi_m$, or equivalently, for ϕ in the range (4.3).

The functions $r(\phi)$ and $s(\phi)$ have hereby been expressed entirely in terms of the coordinates that determine the face. They have been defined sectorwise and at the sector boundaries they are continuous with discontinuous derivatives. After these preliminaries it is now easy to show how they determine the excluded domain.

4.2 Excluded domain \mathcal{V} : a pumpkin

In the vertical half-plane at angle Φ , arc $L_1\tilde{R}L_2$ (of center \mathbf{S}) together with chord L_1L_2 encloses a truncated disk. When Φ is varied, this truncated disk sweeps out the excluded domain \mathcal{V} , that we will now be able to characterize.

⁴Moving, instead, the bisector plane of $L_2\tilde{R}$ away from \mathbf{L}_2 would lead to the same conclusions.

When Φ varies within the m th sector (and hence the local angle ϕ varies from $-\beta_m$ to γ_m), arc $L_1\tilde{R}L_2$ slides along a sphere that has its center in \mathbf{T}_m and whose squared radius is $\overline{OT_m}^2 + L^2$. To see this, it suffices to note that \mathbf{S} is the center of the arc; T_mS is perpendicular to the plane of the arc and hence equidistant to all of its points; and since \mathbf{L}_1 is one of these points, that distance is $(\overline{OT_m}^2 + L^2)^{1/2}$ and independent of S ; hence all arcs have the same distance to \mathbf{T}_m . The surface $\partial\mathcal{V}$ of the excluded domain is therefore piecewise spherical and *the domain \mathcal{V} itself is the union of n balls having their centers in the vertices $\mathbf{T}_1, \dots, \mathbf{T}_n$ of the face.*

In two dimensions, the excluded domain associated with a 2D Voronoi cell is the union of n disks and is often called the *Voronoi flower* of that cell. In the present case the cell face has associated with it a 3D excluded domain \mathcal{V} which is the union of n balls having their centers in the xy plane; and because of the shape of its surface $\partial\mathcal{V}$ this domain rightfully deserves the name *Voronoi pumpkin*. Its intersection with the xy plane is similar to a flower: it is the union of n disks centered on the vertices of the face.

4.3 Large- n limit of \mathcal{V} : a spindle torus

This is too early a stage to take the large- n limit. However, it is now possible for us to look ahead and guess what to expect.

In view of our experience with the 2D Poisson-Voronoi cell it is reasonable to assume that for $n \rightarrow \infty$ the vertices \mathbf{T}_m become dense on a curve that tends towards a circle. In that case the union of balls that constitute the excluded volume will tend to a torus; the major radius of this torus cannot be larger than its minor radius, but we cannot be sure at this point how either will scale with n . Plausible heuristic arguments presented elsewhere [14] indicate that the volume of this torus will approach n/λ .⁵ It will appear at the end of our calculation that in fact for $n \rightarrow \infty$ both radii are $\sim n^{1/3}$ and asymptotically equal to leading order.

4.4 Volume \mathcal{V} of the excluded domain \mathcal{V}

For $n \rightarrow \infty$ the variation of Φ within a sector is of the order of $\sim 2\pi/n$ and we may neglect the ϕ dependence of $r(\phi)$ and $s(\phi)$ within that sector. The volume enclosed between the two vertical half-planes (at angles say Φ_{m-1} and Φ_m) defining the sector, and the sphere centered at \mathbf{T}_m , is then an infinitesimal slice of a spindle torus with major and minor radius equal to $s(\phi)$ and $r(\phi)$, respectively, where $s(\phi) < r(\phi)$. The volume of the excluded domain is therefore the sum of the volumes of these slices.

The volume $V^{\text{sp}}(R_+, R_-)$ of a spindle torus with major radius R_+ and minor radius R_- is given by

$$V^{\text{sp}}(R_+, R_-) = 2\pi^2 R_-^3 g(x), \quad x^2 \equiv 1 - R_+^2/R_-^2, \quad (4.6)$$

⁵A torus whose major radius is smaller than its minor radius is referred to as a *spindle torus*. Its surface is sometimes called an *apple*.

in which

$$g(x) = \frac{1}{\pi} \left[x - \frac{1}{3}x^3 + (\pi - \arcsin x)\sqrt{1-x^2} \right]. \quad (4.7)$$

In the present case we have $R_+ = r(\phi)$ and $R_- = s(\phi)$ whence

$$x^2(\phi) \equiv 1 - \frac{s^2(\phi)}{r^2(\phi)} = \frac{L^2}{r^2(\phi)}. \quad (4.8)$$

The infinitesimal toroidal slice swept out therefore has a volume $2\pi^2 r^3(\phi)g(x(\phi)) \times (\Delta\Phi/2\pi)$, and this should be integrated over Φ to yield the excluded volume \mathcal{V} . This gives

$$\mathcal{V} = \frac{1}{2\pi} \sum_{m=1}^n \int_{-\beta_m}^{\gamma_m} d\phi \, 2\pi^2 r^2(\phi)g(x(\phi)), \quad (4.9)$$

it being understood here and henceforth that under the sum on m the functions $r(\phi)$ and $x(\phi)$ take their expressions valid in the m th angular sector. Eq. (4.9) together with the substitutions (4.5), (4.7), and (4.8) yields the excluded volume in terms of the face coordinates. The m th term in the sum in (4.9) depends on the face coordinates s_{m-1}, s_m, β_m , and γ_m .

We have shown, therefore, that \mathcal{V} depends only on the coordinates $\{\mathbf{S}_1, \dots, \mathbf{S}_n\}$ and on L . The same remark holds for the indicator χ . We will therefore write these two functions from here on as $\mathcal{V}(\mathbf{S}_1, \dots, \mathbf{S}_n; L)$ and $\chi(\mathbf{S}_1, \dots, \mathbf{S}_n; L)$. That is, they are independent of the polar angles θ_m . We are now able to do the integrations on the angles θ_m .

5 Integrating over the polar angles θ_m

We take up again the calculation of $\pi_n(L)$, for which we found expression (3.14). We now exploit the fact just shown that \mathcal{V} and χ are independent of the polar angles θ_m . The polar angle integrations in (3.14) therefore factorize and the one on θ_m becomes

$$\begin{aligned} \int_{-\pi+\delta_m}^{\pi-\delta_m} d\theta_m \left[1 + \frac{\cos \theta_m}{\cos \delta_m} \right]^2 &= \frac{(\pi - \delta_m)(3 - 2 \sin^2 \delta_m)}{\cos^2 \delta_m} + 3 \tan \delta_m \\ &= 3\pi + \pi \tan^2 \delta_m + 3(\tan \delta_m - \delta_m) - \delta_m \tan^2 \delta_m \\ &\equiv 3\pi K\left(\frac{L}{s_m}\right), \end{aligned} \quad (5.1)$$

in which $\cos \delta_m$ is given in terms of L/s_m by (3.12) and where the last line defines $K(x)$, which is such that $K(0) = 1$. We will set

$$e^{\mathcal{K}} = \prod_{m=1}^n K\left(\frac{L}{s_m}\right). \quad (5.2)$$

Upon using (5.1) and (5.2) in (3.14) we find for $\pi_n(L)$ the expression

$$\begin{aligned} \pi_n(L) \simeq & \frac{32\pi\lambda^{n+1}}{c_F} \frac{(3\pi)^n L^2}{n!} \int_0^\infty \left[\prod_{m=1}^n ds_m s_m^2 \right] e^{\mathcal{K}} \\ & \times \int_0^{2\pi} \prod_{m=1}^n d\Phi_m \chi(\mathbf{S}_1, \dots, \mathbf{S}_n; L) e^{-\lambda\mathcal{V}(\mathbf{S}_1, \dots, \mathbf{S}_n; L)}. \end{aligned} \quad (5.3)$$

The problem of calculating $\pi_n(L)$ has hereby been reduced from $3n$ to $2n$ coupled integrations: n radial and n angular ones in the xy plane. In the next sections we will subject Eq. (5.3) to several further transformations, the purpose being to cast it in a form amenable to a large- n expansion.

6 Rewriting the $2n$ integrations in the xy plane

6.1 Transforming the radial integrations

We are motivated by the idea that for any given n -edged face, in the large- n limit the s_m will tend to be close to their m -averaged value. We therefore define the *face radius* \mathbf{s} and relative “radii” σ_m by

$$\mathbf{s} = \frac{1}{n} \sum_{m=1}^n s_m \quad \text{and} \quad s_m = \mathbf{s} \sigma_m, \quad m = 1, 2, \dots, n. \quad (6.1)$$

Note that the m -average \mathbf{s} is still a random quantity that varies from one face to another. For later use we also define variables τ_m by

$$\sigma_m = 1 + \tau_m. \quad (6.2)$$

The σ_m and τ_m satisfy the two equivalent sum rules

$$\sum_{m=1}^n \sigma_m = 1, \quad \sum_{m=1}^n \tau_m = 0. \quad (6.3)$$

When n gets large we expect the σ_m to be close to unity and therefore the τ_m small in a way to be specified quantitatively later.

We may now pass in (5.3) from the n integrations on the s_m to a single integration on \mathbf{s} and n integrations on the σ_m , while introducing a delta function constraint that enforces sum rule (6.3). This converts Eq. (5.3) into

$$\begin{aligned} \pi_n(L) \simeq & \frac{32\pi\lambda^{n+1}}{c_F} \frac{(3\pi)^n L^2}{n!} \int_0^\infty d\mathbf{s} \mathbf{s}^{3n-1} \\ & \times \int_0^\infty \left[\prod_{m=1}^n d\sigma_m \sigma_m^2 K\left(\frac{L}{\mathbf{s}\sigma_m}\right) \right] \delta\left(1 - \frac{1}{n} \sum_{m=1}^n \sigma_m\right) \\ & \times \int_0^{2\pi} \prod_{m=1}^n d\Phi_m \chi(\mathbf{S}_1, \dots, \mathbf{S}_n; L) e^{-\lambda\mathcal{V}(\mathbf{S}_1, \dots, \mathbf{S}_n; L)}. \end{aligned} \quad (6.4)$$

We will now start working on the angular integrations.

6.2 Transforming the angular integrations

We transform the Φ_m integrations in (6.4) in a succession of three steps, largely identical to the procedure followed in Ref. [3]. We therefore indicate these steps only succinctly.

First, we may choose in (6.4) one of the angles Φ_m to be zero, say $\Phi_n = 0$, if we multiply the RHS by 2π to compensate, and we may order the angles according to $0 < \Phi_1 < \Phi_2 < \dots < \Phi_{n-1} < 2\pi$ if we multiply the RHS by $(n-1)!$ to compensate. This ordering makes it convenient to pass from the Φ_m to the angular differences ξ_m (with $m = 1, \dots, n$) defined by

$$\begin{aligned}\xi_m &= \Phi_m - \Phi_{m-1}, & m = 1, \dots, n-1, \\ \xi_n &= 2\pi - \Phi_{n-1}.\end{aligned}\tag{6.5}$$

The geometry imposes the constraints $0 < \xi_m < \pi$ as well as the sum rule $\sum_{m=1}^n \xi_m = 2\pi$.

In the second step we transform for each $m = 1, 2, \dots, n$ separately from the angle ξ_m to the angle β_m defined in figure 3. We observe that

$$\sigma_m = \frac{\cos \gamma_m}{\cos \beta_m} \sigma_{m-1}, \quad m = 1, 2, \dots, n, \quad \sigma_0 \equiv \sigma_n, \tag{6.6}$$

which allows us, under the σ_m integrations in Eq. (6.4), to view γ_m as a function of β_m . Hence we have $\xi_m \equiv \beta_m + \gamma_m = \beta_m + \arccos[(\sigma_m/\sigma_{m-1}) \cos \beta_m]$. The transformation from ξ_m to β_m is therefore accompanied by a Jacobian $j_m \equiv d\xi_m/d\beta_m = \sin(\beta_m + \gamma_m)/[\cos \beta_m \sin \gamma_m]$. The β_m integrals must be appropriately nested. The geometrical condition that the face vertices \mathbf{T}_m have azimuthal angles that increase with m is expressed by the condition $\beta_{m+1} > -\gamma_m$. This is equivalent to imposing the condition expressed by the indicator function χ , which may therefore from here on be omitted. Periodicity is ensured by a factor $\theta(\gamma_n + \beta_1)$, where θ is the Heaviside function.

Thirdly, we introduce extra integrations over the n variables γ_n , compensated by the introduction of a product of Dirac delta functions that impose the n relations (6.6).

Carrying these three steps out leads to

$$\int_0^{2\pi} \prod_{m=1}^n d\Phi_m = 2\pi(n-1)! \int_0^\pi \prod_{m=1}^n d\xi_m \delta\left(\sum_{m=1}^n \xi_m - 2\pi\right) \chi(\mathbf{S}_1, \dots, \mathbf{S}_n; L) \quad (6.7)$$

$$\begin{aligned} &= 2\pi(n-1)! \int_{-\pi/2}^{\pi/2} d\beta_1 \int_{-\gamma_1}^{\pi/2} d\beta_2 \dots \int_{-\gamma_{n-1}}^{\pi/2} d\beta_n \theta(\gamma_n + \beta_1) \\ &\quad \times j_1 j_2 \dots j_n \delta\left(\sum_{m=1}^n (\beta_m + \gamma_m) - 2\pi\right) \end{aligned} \quad (6.8)$$

$$= 2\pi(n-1)! \int d\beta d\gamma \left[\prod_{m=1}^n t_m \sigma_{m-1} \delta\left(\sigma_m - \frac{\cos \gamma_m}{\cos \beta_m} \sigma_{m-1}\right) \right], \quad (6.9)$$

where we define

$$t_m = \frac{\sin(\beta_m + \gamma_m)}{\cos \beta_m \cos \gamma_m} \quad (6.10)$$

and employ the shorthand notation

$$\begin{aligned} \int d\beta d\gamma &= \int_{-\pi/2}^{\pi/2} d\beta_1 \int_{-\beta_1}^{\pi/2} d\gamma_1 \int_{-\gamma_1}^{\pi/2} d\beta_2 \int_{-\beta_2}^{\pi/2} d\gamma_2 \dots \int_{-\gamma_{n-1}}^{\pi/2} d\beta_n \int_{-\beta_n}^{\pi/2} d\gamma_n \\ &\quad \times \theta(\gamma_n + \beta_1) \delta\left(\sum_{m=1}^n (\beta_m + \gamma_m) - 2\pi\right). \end{aligned} \quad (6.11)$$

Eq. (6.9) is to be used to eliminate the Φ_m integrations in (6.4) in favor of the β, γ integrations. Whereas this certainly does not look like a simplification, it is a necessary passage point on the way to our goal.

6.3 Integrating over the radial variables σ_m

Eq. (6.6) relates σ_m to σ_{m-1} . When iterating m times we obtain

$$\sigma_m = \frac{\cos \gamma_m \cos \gamma_{m-1} \dots \cos \gamma_1}{\cos \beta_m \cos \beta_{m-1} \dots \cos \beta_1} \sigma_n, \quad m = 1, 2, \dots, n-1, \quad (6.12)$$

where we recall the convention that $\sigma_0 = \sigma_n$. Let the function G be defined by

$$G(\beta, \gamma) = \frac{1}{2\pi} \sum_{m=1}^n (\log \cos \gamma_m - \log \cos \beta_m). \quad (6.13)$$

Equation (6.12) is valid also when we set $m = n$ and then amounts to a condition on the angles that we have called the *no-spiral constraint*⁶ and that may be expressed as

$$G(\beta, \gamma) = 0 \quad (6.14)$$

⁶The geometrical interpretation leading to this name was given in Ref. [3].

with (β, γ) standing for the set of angles $\{\beta_m, \gamma_m | m = 1, \dots, n\}$. In equation (6.4) we now replace the integration on the angles Φ_m by expression (6.9), interchange the integrations on the β_m and γ_m with those on the σ_m , and carry out the integrals on $\sigma_1, \sigma_2, \dots, \sigma_{n-1}$ with the aid of the delta functions. The integration on σ_n , finally, is easily carried out due to the delta function constraint $\delta(1 - \frac{1}{n} \sum_{m=1}^n \sigma_m)$ in (6.4). The result of all this is that equation (6.4) becomes

$$\begin{aligned} \pi_n(L) \simeq & \frac{32\pi\lambda^{n+1}}{c_F} \frac{(3\pi)^n L^2}{n!} \int_0^\infty ds s^{3n-1} \\ & \times 2\pi(n-1)! \int d\beta d\gamma \frac{\delta(G)}{2\pi} \left[\prod_{m=1}^n \sigma_m^3 t_m \right] e^{\mathcal{K}(\mathbf{s}, \beta, \gamma; L) - \lambda \mathcal{V}(\mathbf{s}, \beta, \gamma; L)} \end{aligned} \quad (6.15)$$

$$= \frac{32\pi\lambda^{n+1}}{c_F} \frac{(3\pi)^n L^2}{n} \int d\beta d\gamma \delta(G) \left[\prod_{m=1}^n \sigma_m^3 t_m \right] I_n(\beta, \gamma; L) \quad (6.16)$$

The σ_m that still appear in (6.15) and (6.16) must now be viewed as functions of the variables of integration determined by the $n-1$ relations (6.12) and sum rule (6.3); we have furthermore abbreviated

$$I_n(\beta, \gamma; L) = \int_0^\infty ds s^{3n-1} e^{\mathcal{K}(\mathbf{s}, \beta, \gamma; L) - \lambda \mathcal{V}(\mathbf{s}, \beta, \gamma; L)}, \quad (6.17)$$

in which we have expressed \mathcal{V} as a function of the new variables of integration using the notation $\mathcal{V}(\mathbf{S}_1, \dots, \mathbf{S}_n; L) = \mathcal{V}(\mathbf{s}, \beta, \gamma; L)$, and where we have shown explicitly the dependence of \mathcal{K} on the same variables. The factor $\delta(G)/2\pi$ in (6.15) and (6.16) enforces the no-spiral constraint (6.14).

Up until this point all transformations of variables applied to the initial expression (2.10) have been exact, with the exception of the discussion in section 3.2.4, where an exponentially small contribution in n was omitted. Eq. (6.16) now expresses $\pi_n(L)$ entirely as an integral over $2n$ angular variables and over the single radial variable \mathbf{s} . In our work [3] on the sidedness problem in 2D a radial integration occurred that could be done almost trivially. Such is not the case here, and from this point on we will have recourse to an expansion in inverse powers of n .

7 Expansion in powers of n

Our approach will consist in finding, in the $2n$ -dimensional phase space, the maximum of the integrand on the RHS of Eq. (6.16), and to show that an expansion about this maximum is possible.

7.1 Scaling with n

In order to carry out a large- n expansion of $\pi_n(L)$ as given by equations (6.16)-(6.17), we hypothesize for the various variables involved in the calculation the

following scaling with n ,

$$\begin{aligned}
r(\phi), s(\phi), s_m, \mathbf{s} &\sim n^{1/3}, \\
L &\sim n^{-1/6}, \\
\tau_m, \beta_m, \gamma_m &\sim n^{-1/2}, \\
\xi_m, \eta_m &\sim n^{-1},
\end{aligned} \tag{7.1}$$

with ξ_m and η_m defined in the caption of figure 3. The scaling of \mathbf{s} and L is suggested by recent work [14], whereas the scaling of the angles β_m and γ_m is taken from reference [3]. The latter implies the scaling of the τ_m *via* equations (6.12) and (6.2). The scaling of the ξ_m and η_m is a consequence of the sum rules $\sum_{m=1}^n \xi_m = \sum_{m=1}^n \eta_m = 0$. Obviously, in each of the two sums $\xi_m = \beta_m + \gamma_m$ and $\eta_m = \gamma_m + \eta_{m+1}$ the order $n^{-1/2}$ contributions must cancel.

We will encounter below many different expressions containing sums of exactly n or of $\mathcal{O}(n)$ terms, where each term is a random variable depending on the β_m and γ_m . It was shown in detail in Ref. [3] how the scaling with n of such sums may be determined. The basic rule is that the sum of $\sim n$ random variables of zero average scales with an extra factor $n^{1/2}$ and the sum of variables of nonzero average with an extra factor n . This rule is complicated by the fact that the averages of β_m and γ_m are $\sim n^{-1}$ but their rms deviations of order $n^{-1/2}$, as well as by the occurrence of products of correlated variables (such as $\tau_m \gamma_m$). Our expansion in negative powers of n will take all this into account, and we will occasionally refer to Ref. [3] for details.

The fact, shown below, that the perturbation expansion leads to a series with finite coefficients will be considered by us as proof of the correctness of the assumed scaling (7.1).

7.2 Expansion of \mathcal{V}

We consider first the pumpkin volume \mathcal{V} whose expression is given by (4.9). The function $g(x)$ occurring there is defined by (4.7) and has the small x expansion

$$g(x) = 1 - \frac{1}{2}x^2 - \frac{1}{8}x^4 + \mathcal{O}(x^5), \tag{7.2}$$

which we will use in equation (4.9). Equations (4.8) and (7.1) show that $x(\phi)$ scales as $\sim n^{-1/2}$, so that (4.9) may be expanded as

$$\mathcal{V} = \frac{1}{2\pi} \sum_{m=1}^n \int_{-\beta_m}^{\gamma_m} d\phi \, 2\pi^2 r^3(\phi) \left[1 - \frac{L^2}{2r^2(\phi)} - \frac{L^4}{8r^4(\phi)} + \mathcal{O}(n^{-3}) \right]. \tag{7.3}$$

We will use the two expressions (4.5) for $r(\phi)$ and expand these in turn, abbreviating $\epsilon_m = \cos^2 \phi / \cos^2 \beta_m - 1$ so that $\epsilon_m \sim L^2/s_{m+1}^2 \sim n^{-1}$. Expanding for large

n we get from the first equality of equation (4.5)

$$\begin{aligned} r(\phi) &= s_{m-1} \left[1 + \frac{1}{2} \left\{ \epsilon_m + \frac{L^2}{s_{m-1}^2} \right\} - \frac{1}{8} \left\{ \epsilon_m + \frac{L^2}{s_{m-1}^2} \right\}^2 + \dots \right] \\ &= s_{m-1} \left[1 + \frac{\epsilon_m}{2} + \frac{L^2}{2s_{m-1}^2} - \frac{\epsilon_m L^2}{4s_{m-1}^2} - \frac{L^4}{8s_{m-1}^4} + \frac{c}{n^2} + \mathcal{O}(n^{-3}) \right], \end{aligned} \quad (7.4)$$

in which we have adopted a convention that we will use repeatedly below: the symbol “ c ” stands for an expression, each time a different one, that may depend on β, γ , and s , is of order n^0 as $n \rightarrow \infty$, but *does not depend on* L . In fact, inside the square brackets in equation (7.4) the second and third term are of order n^{-1} and the fourth and fifth term represent the full L dependent contribution to order n^{-2} .

The second equality of equation (4.5) gives the same result as (7.4) up to the substitutions $s_{m-1} \mapsto s_m$ and $\beta_m \mapsto \gamma_m$. In each sector these two expressions are equivalent. We will find it convenient to use below the first one for $\phi > 0$ and the second one for $\phi < 0$.

After inserting the expansions (7.4) for $r(\phi)$ in (7.3), also expanding ϵ_m to quadratic order in the angles, doing the ϕ integrals, and rearranging terms, we get

$$\mathcal{V} = \frac{1}{2\pi} \sum_{m=1}^n 2\pi^2 s_m^3 \left[\gamma_m + \beta_{m+1} + \gamma_m^3 + \beta_{m+1}^3 + \frac{L^2}{s_m^2} (\gamma_m + \beta_{m+1}) + \frac{c}{n^2} + \mathcal{O}(n^{-3}) \right] \quad (7.5)$$

At order n^{-1} we might have expected terms proportional to L^4 in (7.5), but these appear to cancel. After introducing the variables s and τ_m , and expanding for small τ_m , there appear sums of products of the τ_m, γ_m , and β_m . We define the following expressions that are all of order n^0 as n gets large,

$$\begin{aligned} G_2(\beta, \gamma) &= \frac{n}{2\pi} \sum_{m=1}^n \tau_m (\gamma_m + \beta_{m+1}), \\ F_2(\beta, \gamma) &= \frac{1}{2} \sum_{m=1}^n (\gamma_m^2 + \beta_{m+1}^2), & \tilde{F}_2(\beta, \gamma) &= \frac{n}{6\pi} \sum_{m=1}^n (\gamma_m^3 + \beta_{m+1}^3), \\ F_4(\beta, \gamma) &= \sum_{m=1}^n \tau_m^2, & \tilde{F}_4(\beta, \gamma) &= \frac{n}{2\pi} \sum_{m=1}^n \tau_m^2 (\gamma_m + \beta_{m+1}). \end{aligned} \quad (7.6)$$

We recall here that the τ_m are functions of the β_m and γ_m defined implicitly by (6.2), (6.12), (6.13), and (6.14). Using that $\sum_{m=1}^n (\beta_m + \gamma_m) = 2\pi$ we get from (7.5) and (7.6)

$$\mathcal{V}(s, \beta, \gamma; L) = 2\pi^2 s^3 \left[1 + \frac{L^2}{s^2} + \frac{W}{n} + \frac{L^2}{s^2} \frac{G_2}{n} + \frac{c}{n^2} + \mathcal{O}(n^{-3}) \right]. \quad (7.7)$$

in which

$$W = 3G_2 + 3\tilde{F}_4 + 3\tilde{F}_2. \quad (7.8)$$

The prefactor $2\pi^2 s^3$ in (7.7) is the volume of a torus whose major and minor radius are both equal to s (sometimes called a *horn torus*). With the scaling

assumed in (7.1) this prefactor is $\sim n$ as $n \rightarrow \infty$. Inside the brackets in (7.7), where $L^2/s^2 \sim n^{-1}$, we have included all terms of order n^{-1} , as well as the L dependent term of order n^{-2} . The L independent terms of order n^{-2} are indicated as c/n^2 , where c is left undetermined. At order n^{-1} we might have expected terms proportional to L^4/s^4 and to $(L^2/s^2)(\gamma_m^3 + \beta_m^3)$, but both appear to cancel.

7.3 Expansion of \mathcal{K}

We consider now the quantity $e^{\mathcal{K}}$ that resulted from the integration over the polar angles and is given by (5.2) and (5.1). From Eq. (5.1) we find by straightforward expansion that

$$K(x) = 1 + \frac{1}{3}x^2 + \mathcal{O}(x^5) = \exp \left[\frac{1}{3}x^2 - \frac{1}{18}x^4 + \mathcal{O}(x^5) \right], \quad (7.9)$$

which when substituted in (5.2) leads to

$$\mathcal{K}(s, \beta, \gamma; L) = \frac{nL^2}{3s^2} + \frac{L^2}{s^2}F_4 - \frac{nL^4}{18s^4} + \mathcal{O}(n^{-2}) \quad (7.10)$$

Since $L^2/s^2 \sim n^{-1}$ we see that the first term on the RHS of (7.10) is of order n^0 and the second and third are of order n^{-1} .

7.4 Expansion of $\mathcal{K} - \lambda\mathcal{V}$

Taking (7.7) and (7.10) together we have

$$\begin{aligned} \mathcal{K} - \lambda\mathcal{V} &= -2\pi^2\lambda s^3 \\ &\quad -2\pi^2\lambda sL^2 - 2\pi^2\lambda s^3 \frac{W}{n} + \frac{nL^2}{3s^2} \\ &\quad + \frac{L^2}{s^2}F_4 - \frac{nL^4}{18s^4} - 2\pi^2\lambda sL^2 \frac{G_2}{n} + \frac{c}{n} \\ &\quad + \mathcal{O}(n^{-2}), \end{aligned} \quad (7.11)$$

where we have arranged terms such that the ones in the first, second, and third line are $\mathcal{O}(n)$, $\mathcal{O}(n^0)$, and $\mathcal{O}(n^{-1})$, respectively. To see this it suffices to know that the only hidden factors of n are those in $s^3 \sim n$ and $L^2/s^2 \sim n^{-1}$.

8 Integrating over the face radius s

8.1 The integral $I_n(\beta, \gamma; L)$

We substitute result (7.11) for $\mathcal{K} - \lambda\mathcal{V}$ in the integral $I_n(\beta, \gamma; L)$ defined by (6.17). Let dimensionless scaled variables x and Λ be defined by

$$\begin{aligned} x &= (2\pi^2\lambda)^{1/3}n^{-1/3}s, \\ \Lambda &= (2\pi^2\lambda)^{1/3}n^{1/6}L. \end{aligned} \quad (8.1)$$

In terms of these integral (6.17) may be written

$$I_n = \left(\frac{n}{2\pi^2\lambda}\right)^n \int_0^\infty dx e^{f(x)} \left[1 + \frac{Y_\Lambda(x)}{n} + \frac{c}{n} + \mathcal{O}(n^{-2})\right], \quad (8.2)$$

in which $Y_\Lambda(x)/n$ stands for the sum of the first three terms in the third line of (7.11), that is, in terms of x and Λ ,

$$Y_\Lambda(x) = \frac{\Lambda^2}{x^2} F_4 - \frac{\Lambda^4}{18x^4} - x\Lambda_2 G_2, \quad (8.3)$$

and where we define

$$f(x) = (3n-1)\log x - nx^3 - x^3 W - \Lambda^2 \left(x - \frac{1}{3x^3}\right). \quad (8.4)$$

For $L = 0$, hence $\Lambda = 0$, the integral is easy to calculate in closed form. For the general case $L \geq 0$ we will calculate I_n in the limit of large n , with $L \sim n^{-1/6}$, as stated in our hypothesis (7.1).

8.2 Saddle point expansion

We will carry out the integral (8.2) by means of a saddle point expansion. We calculate the leading order term and the corrections of relative order n^{-1} , limited to those that are dependent on L .

The saddle point condition $df(x)/dx = 0$ applied to (8.4) has the solution $x = x_*$ where

$$x_* = 1 + \frac{x_1}{n} + \frac{x_2}{n^2} + \mathcal{O}(n^{-3}) \quad (8.5)$$

in which

$$x_1 = -\frac{1}{9} - \frac{W}{3} - \frac{5\Lambda^2}{27}. \quad (8.6)$$

The explicit expression for x_2 is easy to find but will drop out of later calculations. Setting $f_* \equiv f(x_*)$ we find by substitution of (8.5) in (8.4) that

$$f_* = -n - W - \frac{2}{3}\Lambda^2 + \frac{9}{2n}x_1^2 + \mathcal{O}(n^{-2}). \quad (8.7)$$

This, combined with (8.6), in turn leads to the expansion

$$e^{f_*} = e^{-n} e^{-W - \frac{2}{3}\Lambda^2} \left[1 + \frac{1}{n} \left(\frac{5}{27}(1+3W)\Lambda^2 + \frac{25}{162}\Lambda^4\right) + \frac{c}{n} + \mathcal{O}(n^{-2})\right], \quad (8.8)$$

where only the Λ dependent terms in x_1^2 have been included explicitly, the remaining ones being absorbed by c . We recall here our convention to let c stand for terms that are of order n^0 but do not depend on Λ , whereas $\mathcal{O}(n^{-k})$ indicates any terms, whether Λ dependent or not, that are of order n^{-k} . For the k th derivative $f_*^{(k)}$ at the saddle point we have

$$\begin{aligned} f_*^{(2)} &= -9n + 1 - 6W + 2\Lambda^2 + \mathcal{O}(n^{-1}), \\ f_*^{(3)} &= \mathcal{O}(n^0), \\ f_*^{(4)} &= -18n + \mathcal{O}(n^0). \end{aligned} \quad (8.9)$$

The $f_*^{(k)}$ with $k \geq 5$ are all of order n but will not be needed in the calculation. In (8.2) we pass to the new variable of integration $u \equiv x - x_*$ and Taylor expand $f(x)$ and $Y_\Lambda(x)$ about $x = x_*$ in powers of u .

$$I_n = \left(\frac{n}{2\pi^2\lambda}\right)^n e^{f_*} \left[1 + \frac{Y_\Lambda(1)}{n} + \frac{c}{n} + \mathcal{O}(n^{-2})\right] \times \int_{-\infty}^{\infty} du e^{\frac{1}{2}u^2 f_*^{(2)}} \left[1 + \frac{1}{24}u^4 f_*^{(4)} + \mathcal{O}(n^{-2})\right] \quad (8.10)$$

The contributions of terms with odd order derivatives under the integral sign vanish by symmetry. Since $f_*^{(2)}$ scales as $\sim n$, it follows that u scales as $n^{-1/2}$ and, in view of (8.9), that $u^4 f_*^{(4)}$ scales as $\sim n^{-1}$. Upon carrying out the u integration in (8.10) we obtain

$$I_n = \left(\frac{n}{2\pi^2\lambda}\right)^n \left[1 + \frac{Y_\Lambda(1)}{n} + \frac{c}{n} + \mathcal{O}(n^{-2})\right] \times \sqrt{\frac{2\pi}{|f_*^{(2)}|}} \exp(f_*) \left[1 + \frac{f_*^{(4)}}{8[f_*^{(2)}]^2} + \mathcal{O}(n^{-2})\right]. \quad (8.11)$$

We have that $f_*^{(4)}/(8|f_*^{(2)}|^2) = -1/(36n) + \mathcal{O}(n^{-2})$, which to leading order is independent of Λ and may therefore be absorbed in the term c/n . After expanding the square root in (8.11),

$$|f_*^{(2)}|^{-1/2} = \frac{1}{3n^{1/2}} \left[1 + \frac{\Lambda^2}{9n} + \frac{c}{n} + \mathcal{O}(n^{-2})\right], \quad (8.12)$$

and using Stirling's formula $(n/e)^n \sqrt{2\pi n} = n! [1 + c/n + \mathcal{O}(n^{-2})]$ we get

$$I_n(\beta, \gamma; L) = \frac{(n-1)!}{3(2\pi^2\lambda)^n} e^{-W - \frac{2}{3}\Lambda^2} \left[1 + \frac{1}{n} (A_2\Lambda^2 + A_4\Lambda^4 + c) + \mathcal{O}(n^{-2})\right] \quad (8.13)$$

in which

$$A_2 = \frac{8}{27} + \frac{2}{3}G_2 + \frac{5}{3}F_2 + \frac{5}{3}\tilde{F}_4 + F_4, \quad A_4 = \frac{8}{81}, \quad (8.14)$$

and where c is a quantity of order n^0 and independent of Λ that we may leave undetermined.

Equations (8.13) and (8.14) complete the calculation of the integral I_n . The β and γ dependence of the result is contained in the quantities W, A_2, A_4 , given by (7.8) and (7.6), and in c .

8.3 Average face radius and approach to a circle

For given edgedness n the integration over the face radius \mathbf{s} , defined by (6.1), has a maximum at $\mathbf{s} = \mathbf{S}_n$. From (8.1) and (8.5) we see that we have, to leading order in n ,

$$\mathbf{S}_n \simeq (2\pi^2\lambda)^{-1/3} n^{1/3}. \quad (8.15)$$

Near the maximum the integrand is a Gaussian of width

$$\begin{aligned}
\langle (s - S_n)^2 \rangle &= (2\pi^2\lambda)^{-2/3} n^{2/3} \langle (x - x^*)^2 \rangle \\
&= (2\pi^2\lambda)^{-2/3} n^{2/3} / |f_*^{(2)}| \\
&= \frac{1}{9} (2\pi^2\lambda)^{-2/3} n^{-1/3}.
\end{aligned} \tag{8.16}$$

Since $\langle (s - S_n)^2 \rangle^{1/2} / S_n \simeq 1/(3n^{1/2})$, the fluctuations about S_n are negligible in the large- n limit and therefore S_n is also the *average* face radius.

We must now investigate the fluctuations of an individual variable s_m , denoting the distance between the center of the face and its m th edge, and the radius s , which is the average of all n such distances [see equation (6.1)]. We find by combining previous results that

$$\frac{1}{n} \sum_{m=1}^n \langle (s_m - s)^2 \rangle = \frac{1}{n} \sum_{m=1}^n \langle s^2 \tau_m^2 \rangle, \tag{8.17}$$

where we used (6.1) and (6.2). Now, knowing that s is strongly peaked around its average S_n , we may, to leading order, take it out of the angular brackets in (8.17). This leads to

$$\frac{1}{n} \sum_{m=1}^n \langle (s_m - s)^2 \rangle = \frac{S_n^2}{n} \sum_{m=1}^n \langle \tau_m^2 \rangle = f_4 \frac{S_n^2}{n} \sim n^{-1/3}. \tag{8.18}$$

This shows that for $n \rightarrow \infty$ the individual s_m all get infinitely sharply peaked around the average S_n , and we may extend (8.15) to

$$\langle s_m \rangle \simeq S_n \simeq (2\pi^2\lambda)^{-1/3} n^{1/3}, \quad m = 1, 2, \dots, n. \tag{8.19}$$

This last equation implies that the shape of the interface tends to a circle of radius S_n as given by (8.15).

9 Transforming the angular averages

Upon substituting equation (8.13) in (6.16) and using (8.1) for Λ we obtain

$$\begin{aligned}
\pi_n(L) &= \frac{32\pi}{3c_F} \frac{(n-1)!}{n} \left(\frac{3}{2\pi} \right)^n \lambda L^2 \int d\beta d\gamma \delta(G) \\
&\times \left[\prod_{m=1}^n \sigma_m^3 t_m \right] e^{-W - \frac{2}{3}\Lambda^2} \left[1 + \frac{\mathcal{R}_\Lambda}{n} + \mathcal{O}(n^{-2}) \right],
\end{aligned} \tag{9.1}$$

with the symbol $\int d\beta d\gamma$ defined in (6.11) and where we have abbreviated

$$\mathcal{R}_\Lambda = A_2 \Lambda^2 + A_4 \Lambda^4 + c. \tag{9.2}$$

The following development closely parallels the one for the 2D Voronoi cell that was carried out in Ref. [3] (see also Ref. [4], Appendices A and B). Our description will therefore be succinct.

Rather than using the set of variables $\{\beta_m, \gamma_m | m = 1, \dots, n\}$ we will employ the sets $\xi \equiv \{\xi_m | m = 1, \dots, n\}$ and $\eta \equiv \{\eta_m | m = 1, \dots, n\}$; these variables have been defined in the caption of figure 3. Inversely, the β_m and γ_m may be expressed in terms of the sets ξ and η and one of the β_m , let us say β_1 . We have

$$\begin{aligned}\beta_m &= \beta_1 - \sum_{\ell=1}^{m-1} (\xi_\ell - \eta_\ell), \\ \gamma_m &= -\beta_1 + \sum_{\ell=1}^{m-1} (\xi_\ell - \eta_\ell) + \xi_m, \quad m = 1, \dots, n.\end{aligned}\tag{9.3}$$

It would seem that β_1 need be given. However, it was shown in Ref. [4] that the no-spiral constraint $G = 0$ of Eq. (6.14) above, when rewritten with the aid of (9.3) in terms of ξ, η , and β_1 , has a unique solution $\beta_1 = \beta_*(\xi, \eta)$. We write

$$\delta(G) = \frac{\delta(\beta_1 - \beta_*)}{G'}\tag{9.4}$$

in which $G' \equiv dG(\xi, \eta; \beta_1)/d\beta_1$ where the derivative is taken at fixed ξ, η .

The ξ_m and η_m are necessarily nonnegative. We abbreviate the integration on them as

$$\int d\xi d\eta = \int_0^\infty \left[\prod_{m=1}^n d\xi_m d\eta_m \right] \delta\left(\sum_{m=1}^n \xi_m - 2\pi\right) \delta\left(\sum_{m=1}^n \eta_m - 2\pi\right).\tag{9.5}$$

The presence of the two delta functions in definition (9.5) has allowed us to take the upper limits of the integrations equal to infinity. We furthermore need conditions on ξ, η that will guarantee that $\beta_m, \gamma_m < \frac{\pi}{2}$. We will represent these conditions by the indicator function

$$\Theta(\xi, \eta) = \prod_{m=1}^n \left[\theta\left(\frac{\pi}{2} - \beta_m\right) \theta\left(\frac{\pi}{2} - \gamma_m\right) \right].\tag{9.6}$$

The change of variables of integration in (9.1) may then be written as

$$\int d\beta d\gamma \delta(G) = \int d\xi d\eta \frac{1}{G'} \Theta(\xi, \eta).\tag{9.7}$$

With the additional definition

$$e^{-\mathbb{V}} = \frac{1}{G'} \prod_{m=1}^n \frac{\sigma_m^3 t_m}{\xi_m} e^{-W}\tag{9.8}$$

we may then rewrite (9.1) as

$$\begin{aligned}\pi_n(L) &= \frac{32\pi}{3c_F} \frac{(n-1)!}{n} \left(\frac{3}{2\pi}\right)^n \lambda L^2 e^{-\frac{2}{3}\Lambda^2} \int d\xi d\eta \xi_1 \xi_2 \dots \xi_n \\ &\times \Theta e^{-\mathbb{V}} \left[1 + \frac{\mathcal{R}_\Lambda}{n} + \mathcal{O}(n^{-2}) \right].\end{aligned}\tag{9.9}$$

Since [4]

$$\mathcal{N} \equiv \int d\xi d\eta \xi_1 \xi_2 \dots \xi_n = \frac{(2\pi)^{3n-2}}{(2n-1)!(n-1)!}, \quad (9.10)$$

we may multiply this quantity into the prefactor on the RHS of (9.9) and rewrite that relation in the compact form

$$\pi_n(L) = \frac{32\pi}{3c_F} \times \frac{2(12\pi^2)^{n-1}}{(2n)!} \times \lambda L^2 e^{-\frac{2}{3}\Lambda^2} \left\langle \Theta e^{-\mathbb{V}} \left[1 + \frac{\mathcal{R}_\Lambda}{n} + \mathcal{O}(n^{-2}) \right] \right\rangle_0, \quad (9.11)$$

in which for any \mathcal{A} the average $\langle \mathcal{A} \rangle_0$ is defined as

$$\langle \mathcal{A} \rangle_0 = \frac{1}{\mathcal{N}} \int d\xi d\eta \xi_1 \xi_2 \dots \xi_n \mathcal{A}. \quad (9.12)$$

We now consider Θ . For large n the angles will all become small: $\xi_m, \eta_m \sim n^{-1}$ and $\beta_m, \gamma_m \sim n^{-1/2}$, and the conditions imposed by Θ are violated with a probability that is exponentially small in n . In our expansion in powers of n we may therefore set $\Theta = 1$. This leads us to rewrite (9.9) as the final result of this section,

$$\pi_n(L) = \frac{32\pi}{3c_F} \times \frac{2(12\pi^2)^{n-1}}{(2n)!} \times \lambda L^2 e^{-\frac{2}{3}\Lambda^2} \langle e^{-\mathbb{V}} \rangle_0 \left[1 + \frac{\langle \mathcal{R}_\Lambda \rangle}{n} + \mathcal{O}(n^{-2}) \right], \quad (9.13)$$

in which for any \mathcal{A} the average $\langle \mathcal{A} \rangle$ is defined as

$$\langle \mathcal{A} \rangle = \frac{\langle \mathcal{A} e^{-\mathbb{V}} \rangle_0}{\langle e^{-\mathbb{V}} \rangle_0}, \quad (9.14)$$

and where \mathbb{V} and \mathcal{R}_Λ are given by (9.8) and (9.2), respectively. At this point we may notice that to leading order, that is, in the absence of the term \mathcal{R}_Λ/n , the Λ (or: L) dependence of $\pi_n(L)$ has been factorized out.

Our initial problem (2.11) was to evaluate $\pi_n(L)$ an integral on n first-neighbor positions $\mathbf{R}_1, \dots, \mathbf{R}_n$, that is, on $3n$ variables. After we carried out in section 5 the integrals over the polar angles $\theta_1, \dots, \theta_n$ there remained $2n$ variables of integration. Subsequent to further transformations and a large n expansion we have, in equation (9.13), arrived at a $2n$ -fold integration on the variables ξ and η , represented by the angular brackets $\langle \dots \rangle$ and $\langle \dots \rangle_0$.

The highly nontrivial fact about equation (9.13) is that $\langle e^{-\mathbb{V}} \rangle_0$ tends to a constant for $n \rightarrow \infty$. We will show this and determine the value of that constant in the next section.

10 Calculation of $\langle e^{-\mathbb{V}} \rangle_0$

It will appear that apart from a change of coefficients the calculation of $\langle e^{-\mathbb{V}} \rangle_0$, with $e^{-\mathbb{V}}$ defined by (9.8), is identical to those that we performed for the two-dimensional Voronoi cell [3] and for a family of line tessellations [6]. We will therefore heavily rely here on this earlier work.

In (9.8) the factor multiplying e^{-W} may be shown by the methods of Ref. [3] to be equal to

$$\frac{1}{G'} \prod_{m=1}^n \frac{\sigma_m^3 t_m}{\xi_m} = \exp \left(-F_2 + \frac{3}{2} F_4 \right) \left[1 + \mathcal{O}(n^{-1/2}) \right], \quad (10.1)$$

with F_2 and F_4 given in (7.6) and where L -independent correction terms of order $n^{-1/2}$ appear

$$\tilde{F}_2 = F_2 + \mathcal{O}(n^{-1/2}), \quad \tilde{F}_4 = F_4 + \mathcal{O}(n^{-1/2}). \quad (10.2)$$

Upon combining (10.1) and (10.2) with (9.8) and (7.8) we find that

$$\mathbb{V} = \mathbf{A} F_2 + 2\mathbf{B} F_4 + 2\mathbf{C} G_2 + \mathcal{O}(n^{-1/2}) \quad (10.3)$$

with

$$\mathbf{A} = 2, \quad \mathbf{B} = \frac{9}{4}, \quad \mathbf{C} = \frac{3}{2}. \quad (10.4)$$

For the 2D Voronoi cell [3] we had at this stage a similar expression but with $\mathbf{A} = \mathbf{B} = \mathbf{C} = 1$, and for the line tessellation problem [6, 7] we had a family of expressions such that $\mathbf{A} = \alpha - 1$, $\mathbf{B} = \frac{1}{4}\alpha^2$, and $\mathbf{C} = \frac{1}{2}\alpha$. Our present problem, equation (10.4), belongs to the same family and has $\alpha = 3$.

We may discuss without extra effort, from here up to and including equation (10.11), the general expression (10.3) with three arbitrary constants \mathbf{A} , \mathbf{B} , and \mathbf{C} . The expressions for G_2 , F_2 , and F_4 have been defined in (7.6) in terms of the variables β_m and γ_m , but may be expressed in terms of the ξ_m and η_m with the aid of (9.3) and the known value $\beta_1 = \beta_*(\xi, \eta)$. Knowing that $\langle \xi_m \rangle_0 = \langle \eta_m \rangle_0 = 2\pi n^{-1}$ we define the scaled deviations from average

$$\delta x_m = n(\xi_m - 2\pi n^{-1}), \quad \delta y_m = n(\eta_m - 2\pi n^{-1}), \quad (10.5)$$

which vary on scale n^0 . Let their Fourier transforms be

$$\hat{X}_q = \frac{1}{2\pi n^{\frac{1}{2}}} \sum_{m=1}^n e^{2\pi i q m/n} \delta x_m, \quad \hat{Y}_q = \frac{1}{2\pi n^{\frac{1}{2}}} \sum_{m=1}^n e^{2\pi i q m/n} \delta y_m, \quad (10.6)$$

where $q = 0, \pm 1, \pm 2, \dots, \pm(\frac{1}{2}n - \frac{1}{2})$ for n odd and $q = 0, \pm 1, \pm 2, \dots, \pm(\frac{1}{2}n - 1), \frac{1}{2}n$ for n even. In terms of these we find from (7.6) that

$$\begin{aligned} F_k &= \sum_{q \neq 0} \frac{1}{q^k} (\hat{X}_q - \hat{Y}_q)(\hat{X}_{-q} - \hat{Y}_{-q}) + \mathcal{O}(n^{-1/2}), \\ G_2 &= \sum_{q \neq 0} \frac{1}{2q^2} (\hat{X}_q \hat{Y}_{-q} + \hat{X}_{-q} \hat{Y}_q - 2\hat{Y}_q \hat{Y}_{-q}) + \mathcal{O}(n^{-1/2}). \end{aligned} \quad (10.7)$$

It is useful to set $\hat{\mathbf{Z}}_q = (\hat{X}_q, \hat{Y}_q)$. Using (10.7) and (10.2) we may then write (10.3) as

$$\mathbb{V} = \sum_{q \neq 0} \hat{\mathbf{Z}}_q \cdot \mathbf{V}_q \cdot \hat{\mathbf{Z}}_{-q}^T + \mathcal{O}(n^{-1/2}), \quad (10.8)$$

where T stands for transposition and where \mathbf{V}_q is the symmetric matrix

$$\mathbf{V}_q = \begin{pmatrix} Aq^{-2} + 2Bq^{-4} & -(A - C)q^{-2} - 2Bq^{-4} \\ -(A - C)q^{-2} - 2Bq^{-4} & (A - 2C)q^{-2} + 2Bq^{-4} \end{pmatrix}. \quad (10.9)$$

Let $\mathbf{1} = \text{diag}\{1, 1\}$ and $\mathbf{E} = \text{diag}\{1, 2\}$. We define

$$\begin{aligned} \Lambda_q &= \det(\mathbf{1} + \mathbf{V}_q \mathbf{E}) \\ &= 1 + \frac{3A - 4C}{q^2} + \frac{6B - 2C^2}{q^4}. \end{aligned} \quad (10.10)$$

For the general \mathbb{V} given by (10.8) and (10.9), and using definition (9.12) of the average $\langle \dots \rangle_0$, we may show by the methods of Ref. [3] that

$$\langle e^{-\mathbb{V}} \rangle_0 = \prod_{q=1}^{\infty} \Lambda_q^{-1} + \mathcal{O}(n^{-1/2}), \quad n \rightarrow \infty. \quad (10.11)$$

It was certainly not *a priori* evident that this quantity is a finite constant in the limit $n \rightarrow \infty$. The first result of this kind [3] was derived for the 2D Poisson-Voronoi cell.

We return now to the special values (10.4) of A , B , and C relevant to our problem. For these we define $C(3) \equiv \lim_{n \rightarrow \infty} \langle e^{-\mathbb{V}} \rangle_0$, and since in this special case $\Lambda_q = 1 + 9q^{-4}$ we have from (10.11)

$$C(3) = \prod_{q=1}^{\infty} \frac{q^4}{q^4 + 9} = 0.053891. \quad (10.12)$$

This product on the wavenumbers q has the interpretation of a partition function, namely the one of the “elastic” deformations of the n -edged face with respect to a circle, the elasticity being, of course, of purely entropic origin.

11 Calculation of $\langle \mathcal{R}_\Lambda \rangle$

The work that remains to be done is the calculation of the coefficient $\langle \mathcal{R}_\Lambda \rangle$ in (9.13). Obviously it suffices to find its limiting value as $n \rightarrow \infty$.

Although the variables of integration are not Gaussian, it was shown in Ref. [3] that *to leading order in the large- n expansion* averages of type (9.12) may be carried out as if the ξ_m and η_m were distributed with the Gaussian weights

$$\begin{aligned} \frac{1}{\mathcal{N}} \int d\xi d\eta \, \xi_1 \xi_2 \dots \xi_n \mathcal{A} = \\ \int \prod_q d\hat{X}_q d\hat{Y}_q \exp \left(- \sum_{q \neq 0} \hat{X}_q \hat{X}_{-q} - \frac{1}{2} \sum_{q \neq 0} \hat{Y}_q \hat{Y}_{-q} \right) \mathcal{A} + \mathcal{O}(n^{-1/2}) \end{aligned} \quad (11.1)$$

The variances of the \hat{X}_q and the \hat{Y}_q in (11.1) differ by a factor of two due to the appearance of the product $\xi_1 \xi_2 \dots \xi_n$ in the integration on the LHS. The delta function constraints present in the definition (9.5) of $\int d\xi d\eta$ have been incorporated in (11.1): this Gaussian weight does not depend on \hat{X}_0 and \hat{Y}_0 , and neither should the otherwise arbitrary integrand \mathcal{A} .

It was shown in Ref. [3] how correlations between the \hat{X}_q and \hat{Y}_q may be calculated to leading order in the large- n expansion. For \mathbb{V} given by the general expression (10.8)-(10.9) we obtain by the same method the basic correlations

$$\begin{aligned}\langle \hat{X}_q \hat{X}_{-q} \rangle &= \frac{1}{2} - \frac{1}{2\Lambda_q} \left[\frac{\mathbf{A}}{q^2} + \frac{2(\mathbf{B} - \mathbf{C}^2)}{q^4} \right] + \mathcal{O}(n^{-1/2}), \\ \langle \hat{Y}_q \hat{Y}_{-q} \rangle &= 1 - \frac{2}{\Lambda_q} \left[\frac{\mathbf{A} - 2\mathbf{C}}{q^2} + \frac{2\mathbf{B} - \mathbf{C}^2}{q^4} \right] + \mathcal{O}(n^{-1/2}), \\ \frac{1}{2} [\langle \hat{X}_q \hat{Y}_{-q} \rangle + \langle \hat{X}_{-q} \hat{Y}_q \rangle] &= \frac{1}{\Lambda_q} \left[\frac{\mathbf{A} - \mathbf{C}}{q^2} + \frac{2\mathbf{B}}{q^4} \right] + \mathcal{O}(n^{-1/2}).\end{aligned}\quad (11.2)$$

We need the average $\langle \mathcal{R}_\Lambda \rangle$ with \mathcal{R}_Λ given by (9.2), (8.14), and (10.7). Let us set

$$f_k = \lim_{n \rightarrow \infty} \langle F_k \rangle \quad k = 2, 4, \quad g_2 = \lim_{n \rightarrow \infty} \langle G_2 \rangle. \quad (11.3)$$

After Fourier transforming the expressions for F_2, F_4 , and G_2 , then using the basic correlations (11.2), and finally substituting our particular values (10.4) of \mathbf{A}, \mathbf{B} , and \mathbf{C} we obtain

$$f_2 = \frac{3}{2} \sum_{q=1}^{\infty} \frac{q^2}{9 + q^4} = 0.96119, \quad f_4 = \frac{3}{2} \sum_{q=1}^{\infty} \frac{1}{9 + q^4} = 0.23764, \quad (11.4)$$

and $g_2 = -\frac{2}{3}f_2 - f_4$. If we set $a_2 = \langle A_2 \rangle$, $a_4 = A_4$, and $c_0 = \langle c \rangle$, then Eq. (9.2) becomes

$$\langle \mathcal{R}_\Lambda \rangle = a_2 \Lambda^2 + a_4 \Lambda^4 + c_0 \quad (11.5)$$

in which, after elimination of g_2 and with the aid of (11.4),

$$a_2 = \frac{8}{27} + \frac{11}{9}f_2 + 2f_4 = 1.94635, \quad a_4 = \frac{8}{81} = 0.09877, \quad (11.6)$$

and where c_0 has not been calculated. Substituting (11.5) in (9.13) yields

$$\begin{aligned}\pi_n(L) &= \frac{32\pi}{3c_F} \frac{2(12\pi^2)^{n-1}}{(2n)!} C(3) \lambda L^2 e^{-\frac{2}{3}\Lambda^2} \\ &\quad \times \left[1 + \frac{c'_0}{n^{1/2}} \frac{1}{n} \left(a_2 \Lambda^2 + a_4 \Lambda^4 + c_0 + \mathcal{O}(n^{-2}) \right) \right],\end{aligned}\quad (11.7)$$

in which c'_0 is an unknown but Λ -independent coefficient. We suspect that in fact $c'_0 = 0$, mainly because in the related 2D sidedness problem numerical evidence [4] convincingly shows the absence of correction terms of relative order $n^{-1/2}$. Eq. (11.7) is close to our final result.

12 Final results for p_n and $Q_n(L)$

We are now able to list our principal results. We factorize $\pi_n(L)$ according to

$$\pi_n(L) = Q_n(L)p_n, \quad (12.1)$$

where p_n is the probability for the face to have n edges and $Q_n(L)$ is the conditional probability distribution of L for given n . Let us define the dimensionless scaling variable y by

$$\begin{aligned} y = \kappa n^{1/6} L, \quad \kappa &= 2^{-1/6} 3^{-1/2} \pi^{7/6} \lambda^{1/3} \\ &= 1.95558 \lambda^{1/3}, \end{aligned} \quad (12.2)$$

in which the choice of the inverse length constant κ will become clear below. We may eliminate Λ and L from (11.7) in favor of y using (12.2) and the relation $\Lambda = (6/\pi)^{1/2} y$ which follows from (12.2) and (8.1). This leads to

$$p_n = \frac{1}{c_F} \left(\frac{3}{2\pi^5 n} \right)^{1/2} \left[\frac{(12\pi^2)^n}{(2n)!} C(3) \right] \left[1 + \frac{c'_0}{n^{-1/2}} + \frac{c_0}{n} + \mathcal{O}(n^{-2}) \right] \quad (12.3)$$

and

$$\begin{aligned} Q_n(L) dL &= Q_n(y) dy \\ &= Q(y) \left[1 + \frac{1}{n} (q_2 y^2 + q_4 y^4 - q_0) + \mathcal{O}(n^{-2}) \right] dy, \end{aligned} \quad (12.4)$$

in which the first line defines $Q_n(y)$, where $Q(y)$ stands for the probability distribution

$$Q(y) = \frac{32y^2}{\pi^2} \exp\left(-\frac{4y^2}{\pi}\right), \quad y > 0, \quad (12.5)$$

and where

$$q_2 = \frac{6a_2}{\pi} = 3.71726, \quad q_4 = \frac{32}{9\pi^2} = 0.36025. \quad (12.6)$$

The coefficient q_0 in (12.4) is determined by the normalization condition imposed on $Q_n(L)$ to order n^{-1} , which leads to a redefinition of the unknown constant c_0 in (12.3). Using that $\overline{y^2} = 3\pi/8$ and $\overline{y^4} = 15\pi^2/64$ we get

$$q_0 = \frac{9}{4} a_2 + \frac{5}{6} = 5.21263. \quad (12.7)$$

The definition of κ in (12.2) is such that $\overline{y} = 1$, where the overbar denotes the average with respect to $Q(y)$. The higher moments, some of which are needed below, are given by $\overline{y^k} = (\pi/4)^{(k-1)/2} \Gamma((k+3)/2)$.

The important point is that L scales as $\sim n^{-1/6}$ and that its probability distribution is fully known, including the leading correction-to-scaling term. We now recall equations (8.16) and (8.18), which say that this scale $n^{-1/6}$ is also the scale of the root-mean-square *fluctuations* $\langle (s - S_n)^2 \rangle^{1/2}$ and $\langle (s_m - s)^2 \rangle^{1/2}$ associated with the cell radius.

12.1 The average L_n and approach to a horn torus

It follows from (12.4) that the average of L for given n , to be denoted as $L_n \equiv \int_0^\infty dL L Q_n(L)$, behaves asymptotically as

$$\begin{aligned} L_n &= \frac{1}{\kappa n^{1/6}} \left[\bar{y} + \frac{1}{n} \left(q_2 \bar{y}^3 + q_4 \bar{y}^5 - q_0 \bar{y} \right) + \mathcal{O}(n^{-2}) \right] \\ &= \frac{1}{\kappa n^{1/6}} \left[1 + \frac{3a_2 + 2}{4n} + \mathcal{O}(n^{-2}) \right], \end{aligned} \quad (12.8)$$

where in passing from the first to the second line we inserted the explicit expressions $\bar{y} = 1$, $\bar{y}^3 = \pi/2$ and $\bar{y}^5 = 3\pi^2/8$. Using finally equations (11.6) and (11.4) we may render the coefficient a_2 more explicit and (12.8) becomes

$$L_n = \frac{1}{\kappa n^{1/6}} \left[1 + \frac{l_1}{n} + \mathcal{O}(n^{-2}) \right] \quad (12.9)$$

with κ given by (12.2) and in which

$$l_1 = \frac{13}{18} + \frac{1}{8} \sum_{q=1}^{\infty} \frac{18 + 11q^2}{9 + q^4} = 1.95977. \quad (12.10)$$

We now recall relation (3.10),

$$s_m^2 = r_m^2 - L^2, \quad m = 1, 2, \dots, n \quad (12.11)$$

(see Fig. 2). Since s_m gets sharply peaked around $S_n \sim n^{1/3}$ and L_n is of order $n^{-1/6}$, we conclude that r_m must be sharply peaked around a value that we will denote by R_n and that is equal to S_n . That is, because of (8.15),

$$R_n \simeq S_n \simeq (2\pi^2 \lambda)^{-1/3} n^{1/3}. \quad (12.12)$$

Since S_n and R_n are the major and minor radius, respectively, of the limit torus, their equality in the limit $n \rightarrow \infty$ implies that the excluded domain tends to a horn torus, that is, a doughnut with a hole of zero diameter. This conclusion was first reached by Hilhorst and Lazar [14] on the basis of a heuristic theory and of simulations that extended initial work due to Lazar *et al.* [15]. We will now make a brief comparison with that work.

12.2 Comparison to the “entropy *vs.* entropy” theory

An alternative but heuristic approach to the study of various statistical properties of Voronoi cells is based on an “entropy *versus* entropy” argument. The heuristic theory was initially applied to the n -sided 2D Poisson-Voronoi cell [16], for which several of its results turned out to be exact, in particular those for the scaling of the mean cell radius with n . This approach was then generalized [17] to the 3-dimensional n -faced Voronoi cell, which in the limit $n \rightarrow \infty$ becomes a sphere.

However, the n -edged face between adjacent 3D cells has, in the large- n limit, no spherical but merely axial symmetry. For this reason the heuristic theory for the face [14], depends on an additional assumption.

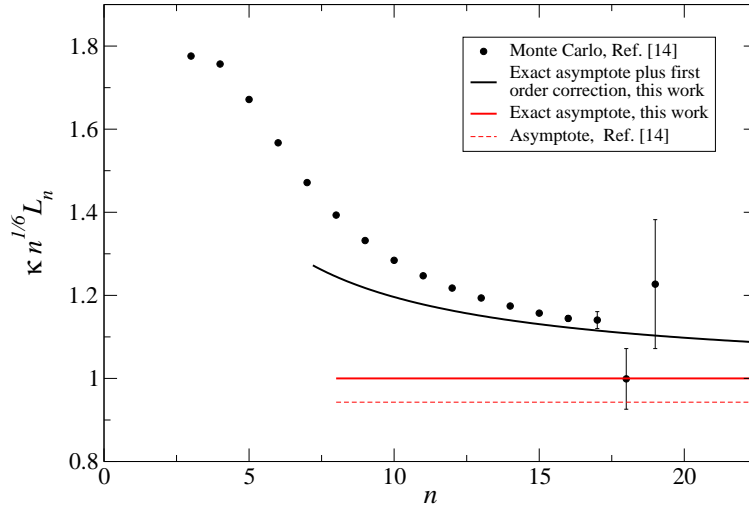


Figure 4: Average focal distance L_n as a function of n . Black dots: Monte Carlo data of Ref. [14]. Solid black curve: prediction of this work, including the $\mathcal{O}(1/n)$ correction to the exact asymptotic behavior. Solid red curve: exact asymptotic limit. Dashed red curve: asymptotic limit according to the heuristic theory of Ref. [14].

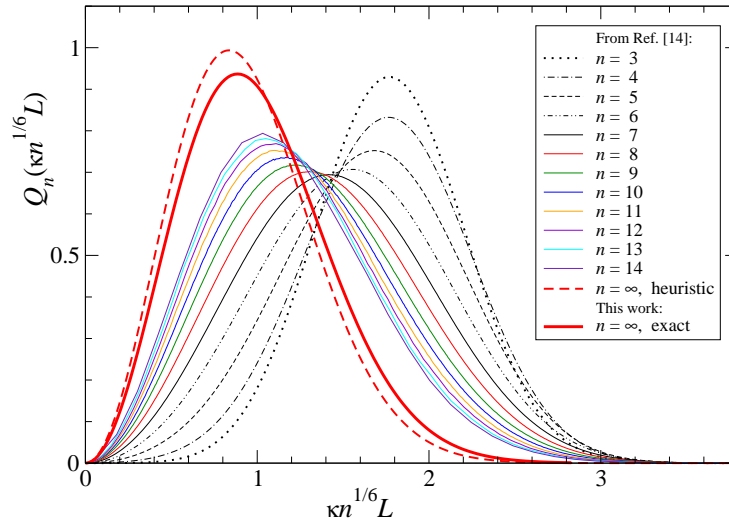


Figure 5: Heavy red solid curve: limit distribution $Q(y)$ of the scaled focal distance $y = \kappa n^{1/6} L$ as $n \rightarrow \infty$ [Eqs. (12.5) and (12.2)]. Heavy red dashed curve: prediction of the heuristic theory of Ref. [14]. Other curves: Monte Carlo results [14] for the finite- n distributions $Q_n(y)$ for $n = 3, 4, \dots, 14$.

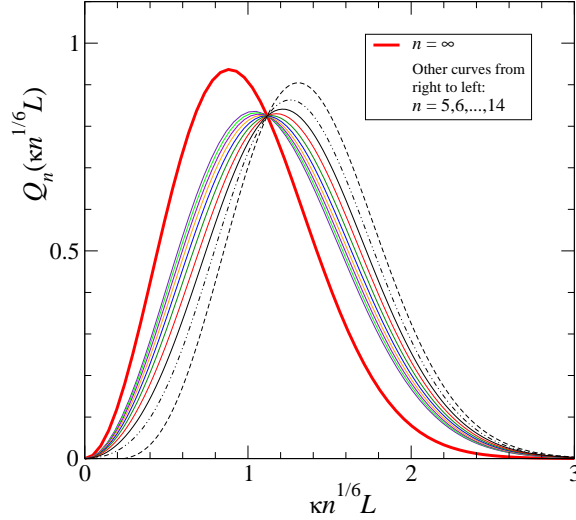


Figure 6: Heavy red solid curve: same as in figure 5. Other curves: the distributions $Q_n(y)$ according to Eq. (12.4) for $n = 5, 6, \dots, 14$ (same color code as in figure 5). See text for further comments.

The exact results found in this work now allow us to assess the validity of the heuristic theory.

(i) The exact asymptotic n dependence of R_n and S_n [Eq. (12.12)] coincides with the results of the heuristic theory of Ref. [14].

(ii) The exact asymptotic n dependence of L_n [Eq. 12.9] has the same power $-1/6$ as found heuristically; however, the exact prefactor $\kappa^{-1} = 0.511357\lambda^{-1/3}$ [Eq. (12.2)] is larger than the heuristic one by a factor of $\sqrt{9/8} = 1.06$.

(iii) The exact function $Q(y)$ that describes the asymptotic probability distribution of L [Eq. (12.5)] is the same as the heuristic one up to a scaling with the same factor $\sqrt{9/8}$ (see figure 5). It is remarkable, since this was unforeseeable, that the heuristic theory for the distribution of y should be so close to being exact.

Our present results go beyond those predicted by the heuristic theory, in particular in that they provide, in Eqs. (12.4) and (12.9), the leading order finite- n corrections to the distribution function $Q(y)$ and to the average L_n , respectively. In the next subsection we will compare these new results to earlier Monte Carlo simulations.

12.3 Comparison to Monte Carlo work

We consider the average focal distance L_n and refer to Figure 4. The Monte Carlo data [14] for this quantity are accurate up to about $n \lesssim 17$. They show appreciable finite- n deviations from the heuristically predicted asymptotic large- n behavior (the dashed red line). This work brings theory and simulations much closer together. First of all, the exact asymptote (solid red line) is higher than the heuristic one by the factor $\sqrt{9/8}$ discussed above. Furthermore, inclusion of the $\mathcal{O}(1/n)$ cor-

rection term [see Eqs. (12.9)-(12.10)] greatly improves the correspondence between theory and simulations.

We now turn to the probability distributions $Q_n(L)$ themselves, or rather their scaled equivalents $Q_n(\kappa n^{1/5}L)$. In Fig. 5 Monte Carlo data [14] are shown for Q_n with $n = 3, 4, \dots, 14$. The exact limiting curve for $n \rightarrow \infty$ [Eq. (12.5)] is the solid black line. The heuristic theory predicted the dashed red curve. Although the exact limit is closer to the finite- n Monte Carlo data, there are still considerable finite size effects for the value of n attainable by the simulations.

In Fig. 6 we show the distributions $cQ_n(y)$ for $n = 5, 6, \dots, 14$ based on Eq. (12.4), and incorporating the correction term of order n^{-1} . The agreement with the Monte Carlo data is qualitative: as n increases, the average L_n goes down while the distribution first gets wider and then narrower again, which has the consequence that the peak value passes through a minimum. Quantitative agreement gets better as n gets large, but finite size effect remain clearly visible.

13 Conclusion

This work represents a new contribution to the statistics of Poisson-Voronoi tessellations in three dimensions.

We have studied an arbitrary face shared by two neighboring cells, the “focal cells.” We determined the probability p_n for this face to have exactly n edges, as well as the conditional probability distribution $Q_n(L)$ of the focal distance L (*i.e.* half the distance between the seeds of the focal cells) given the edgedness n . Calculating these quantities amounts to solving a problem of n interacting particles, and we have shown that this problem may be brought under full control in the limit $n \rightarrow \infty$.

The analytic methods of this paper were developed initially within the context of several two-dimensional problems in random geometry. We have extended them here for the first time to a problem in three dimensions.

Our results, summarized at the end of the introduction, include expressions for the asymptotic $n \rightarrow \infty$ behavior of p_n and $Q_n(L)$. The focal distance L was shown to scale as $n^{-1/6}$ with corrections of relative order $1/n$ whose amplitude was determined. The agreement between the present theory and earlier Monte Carlo simulations is good.

The positions of the edges of the n -edged face are determined by the positions of n first-neighbors seeds to the pair of focal seeds. These first neighbors were shown to lie, for large n , on the surface of a spindle torus whose interior excludes all seeds other than the two focal seeds. For $n \rightarrow \infty$ the major and minor radii of this torus (that were shown to scale as $n^{1/3}$) become equal: the limit of the excluded domain is a doughnut with a zero diameter hole.

We conclude by mentioning again the closely related problem that comes naturally to mind, *viz.*, to find, for asymptotically large n , the probability $p_n^{(3)}$ that a three-dimensional Poisson-Voronoi cell have n faces. In spite of the progress achieved here, that question remains an open challenge.

References

- [1] A. Okabe, B. Boots, K. Sugihara, and S. N. Chiu, *Spatial tessellations: concepts and applications of Voronoi diagrams*, second edition (John Wiley & Sons Ltd., Cichester, 2000).
- [2] H.J. Hilhorst, *J. Stat. Mech.* (2005) L02003.
- [3] H.J. Hilhorst, *J. Stat. Mech.* (2005) P09005.
- [4] H.J. Hilhorst, *J. Phys. A: Math. Theor.* **40** (2007) 2615.
- [5] H.J. Hilhorst, *J. Phys. A: Math. Theor.* **39** (2006) 7227.
- [6] H.J. Hilhorst and P. Calka, *J. Stat. Phys.* **132** (2008) 627-647.
- [7] D. Hug and R. Schneider, *Geom. Funct. Anal.* **17**, 156 (2007).
- [8] H.J. Hilhorst, P. Calka, and G. Schehr, *J. Stat. Mech.* (2008) P10010.
- [9] J. J. Sylvester, *Problem 1491, The Educational Times* (College of Preceptors, London) April 1864.
- [10] Th. W. Burkhardt, *J. Stat. Mech.* (2007) P07004
- [11] S.N. Majumdar, A. Rosso, and A. Zoia, *J. Phys. A: Math. Theor.* **43** (2010) 115001
- [12] A. Reymbaut, S.N. Majumdar, and A. Rosso, *J. Phys. A: Math. Theor.* **44** (2011) 415001.
- [13] S. Kumar, S.K. Kurtz, J.R. Banavar, and M.G. Sharma, *J. Stat. Phys.* **67** (1992) 523.
- [14] H.J. Hilhorst and E.A. Lazar, *J. Stat. Mech.* (2014) P10021.
- [15] E.A. Lazar, J.K. Mason, R.D. MacPherson, and D.J. Srolovitz, *Phys. Rev. E* **88**, 063309 (2013).
- [16] H.J. Hilhorst, *J. Stat. Mech.* (2009) P05007.
- [17] H.J. Hilhorst, *J. Stat. Mech.* (2009) P08003.